NASA’s Planetary Science Missions Present and Future Plans

*James L Green[1]

1. NASA Headquarters

Planetary Science missions have revolutionized our understanding of the origin and evolution of the solar system. Planetary scientists are also enabling human space exploration by studying and characterizing planetary environments beyond Earth and identifying possible resources that will enable safe and effective human missions to destinations beyond low Earth orbit. Robotic explorers are gathering data to help us understand how the planets formed, what triggered different evolutionary paths among planets, what processes are active, and how the Earth formed, evolved, and became habitable. To search for evidence of life beyond Earth, we’ve used this data to map zones of habitability, studied the chemistry of unfamiliar worlds, and revealed the processes that lead to conditions necessary for life. In addition, we have significantly increased our ability to detect, track, catalog, and characterize near-Earth objects that may either pose hazards to Earth or provide destinations and resources for future exploration.

NASA’s Planetary Science Division (PSD) and space agencies around the world are collaborating on an extensive array of missions exploring our solar system. NASA has always encouraged international participation on our missions both strategic and competitive and other Space Agencies have reciprocated and invited NASA investigators to participate in their missions.

NASA PSD has a fleet of assets and partnerships that are focused on the exploration and understanding of the Solar System. Indeed, we are living in a golden age of discovery with a large number of operating missions ranging from orbiting Mercury to heading for beyond Pluto.

In my talk I will present an overview of current and possible future PSD missions. As we have we just launched OSIRIS-Rex, and announced the Discovery Program selections, we continue the implementation of the New Frontiers mission and the InSight mission. As our present fleet of missions continue to provide immense amounts of data from the Moon, Mars, and all the way to Pluto, we continue work to deliver NASA's contributions to fly on international missions such as ESA's JUICE mission consisting of one U.S.-led science instrument and hardware for two European instruments: the radar, ultraviolet spectrometer, and the particle environment package.

Future NASA Mars missions include NASA’s InSight lander designed to study the Mars interior and the Mars 2020 rover that will produce rock cores from a geologically diverse sight for potential future return. In addition to the strong international scientific program at Mars, NASA is developing the capabilities needed to send humans to Mars in the 2030s and beyond.

The exploration of the outer Solar System has recently revealed remarkable information regarding “ocean worlds” such as Europa and Enceladus, which have oceans or seas of liquid water beneath their icy surfaces. The Cassini mission has discovered vast oceans of liquid hydrocarbons on Saturn’s moon Titan and a submerged salt-water sea on Saturn’s moon Enceladus. Titan also has seas and lakes of liquid methane/ethane on its surface. With these new discoveries, small worlds have become a primary focus in the search for possible life elsewhere in the Solar System.

But regardless of the destination, international partnerships are an excellent, proven way of amplifying the

scope and sharing the science results of a mission otherwise implemented by an individual space agency. The exploration of the Solar System is uniquely poised to bring planetary scientists, worldwide, together under the common theme of understanding the origin, evolution, and bodies of our solar neighborhood. In the past decade we have witnessed great examples of international partnerships that made various missions the success they are known for today. As Director of Planetary Science at NASA I will continue to seek cooperation with our strong international partners in support of planetary missions.

Keywords: NASA, Planetary, Missions, International

JUICE/GALA-J (1) : The Ganymede Laser Altimeter (GALA) for the JUICE mission - Introduction and current status

*Keigo Enya[1], Noriyuki Namiki[2], Masanori Kobayashi[3], Jun Kimura[4], Hirotomo Noda[2], Hiroshi Araki[2], Shingo Kashima[2], makoto Utsunomiya[2], Katsuhiko Ishibashi[3], Shingo Kobayashi[6], Shoko Oshigami[5], Takahide Mizuno[1], Masanobu Ozaki[1], Toshihiko Yamawaki[1], Kazuyuki Touhara[1], Yoshifumi Saito[1], Shunichi Kamata[7], Koji Matsumoto[2], Kiyoshi Kuramoto[7], Sho Sasaki[4], Satoru Iwamura[8], Teruhito Iida[9], Naofumi Fujishiro[10], Masayuki Fujii[11], Hauke Hussmann[12], Kay Lingenauber[12], Reinald Kallenbach[12], Judit Jaenchen[12], Thomas Behnke[12], Christian Althaus[12], Simone DelTogno[12], Juergen Oberst[12], Horst-Georg Loetzke[12], Harald Michaelis[12]

1. ISAS, 2. NAOJ, 3. CIT, 4. Osaka University, 5. Kogakuin University, 6. NIRS, 7. Hokkaido University, 8. MRJ, 9. PLANET, 10. astroopt, 11. Meisei Electric, 12. DLR

We present an introduction, current status, and role of the Japan team for the Ganymede Laser Altimeter (GALA) for the Jupiter Icy Moon Explorer (JUICE) mission. JUICE is a mission of ESA to be launched in 2022, and GALA is one of the payloads of JUICE.

Major objectives of GALA are to provide topographic data of Ganymede, the largest satellite of Jupiter, and to measure its tidal amplitudes. The latter is crucially important to detect and to characterize an underground ocean on Ganymede. Furthermore, GALA support geological studies, e.g., identification of characterization of tectonic and cryo-volcanic regions, impact basins, and craters. GALA also provides information on surface roughness and the albedo.

For the laser altimetry, GALA emits and receives laser pulses at about 500 km altitude above Ganymede. Wavelength, energy, and repetition frequency of the laser plus are 1064 nm, 17 mJ, and 30 Hz, respectively. Reflected beam from the Ganymede surface is received by the receiver telescope with 25 cm diameter aperture, re-focused by the BEO including a narrow band-pass filter, and then detected by the APD detector.

Development of GALA is carried out in international collaboration from Germany, Japan, Switzerland, and Spain. GALA-Japan will develop the Backend Optics (BEO), the Focal Plane assembly (FPA) including an avalanche photo-diode (APD) detector, and the Analog Electronics module (AEM) in the receiver chain.Development of hardware, the structure and thermal models and following models, was started. In the presentation, we will report the newest project status updated for the conference date.

Keywords: JUICE, GALA, Jupiter, Ganymede, Laser altimeter

Variations of Io's volcanic activity seen in Jupiter's extended sodium nebula

*Mizuki Yoneda[1], Fuminori Tsuchiya[2], Masato Kagitani[2], Katherine De Kleer[3], Takeshi Sakanoi[2]

1. Kiepenheuer Institute for Solar Physics, 2. Tohoku Universiy, PPARC, 3. University of California, Berkeley

Io, which is one of the Galilean moons of Jupiter, is the most volcanically active body in the Solar System. Volcanic atmosphere is ionized and picked-up by Jupiter's co-rotating magnetic fields. This plasma distributes in Jupiter's inner magnetosphere and forms a structure called Io plasma torus. Major constituents in the torus are sulfur and oxygen ions, and most of these ions have emissions lines at UV wavelengths. Although this is a minor constituent, NaCl+ should be included in the torus since Cl+ ions was detected from the ground, and neutral sodium atoms show the most distinct emission at sodium D-line wavelengths in the torus. Not only in the torus, sodium emission can be observed also in a vast region whose extent is 1,000 Juipter's radii around Jupiter. This structure is called Jupiter's sodium nebula, or Mendillo-sphere. This means these sodium atoms have enough velocity to escape from Jupiter's and Io's gravitational-spheres.

These sodium atoms seem to be originated from sodium chloride in Io's volcanic gas. This gas becomes Io's ionospheric plasma. Pick-up of these NaCl+ ions from Io's ionosphere and their subsequent destruction in the plasma torus produces fast from of neutral sodium atoms, then Jupiter's sodium nebula is formed. This sodium nebula can be observed from the ground using small telescopes.

We have been making observations of Jupiter's sodium nebula atop Heleakala in Maui island, Hawaii, and found the nebula shows variations that seem to correspond to those in Io's volcanic activity. Since 2013, we have been making the observations in conjunctions with the Hisaki and Juno spacecraft. The most distinct event during this campaign was seen in 2015. Other than this, several minor enhancements were observed.

In this presentation, we will show latest sodium data that is representative of Io's volcanism. Also, comparisons of the sodium data with Hisaki’ s torus data and Io's infrared observations will be shown.

Keywords: Io, Jupiter, volcanism

A Survey of D-type Spectra on the Moon based on Hyperspectral Remote Sensing

*Satoru Yamamoto[1], Sei-ichiro WATANABE[2], Tsuneo Matsunaga[1]

1. National Institute for Environmental Study, 2. Nagoya University

Spectral D-type asteroids are characterized by dark, red-sloped, and featureless spectra in the visible and near-infrared wavelengths, and are though to be composed of rocks rich in organic compounds. The Martian two satellites, Phobos and Deimos, resemble spectrally D-type asteroids, suggesting that their origins are by capture of D-type asteroids outside the Martian system, while we need to explain how they were captured and evolved into near-circular and equatorial orbits around the Mars. Alternative explanation is that the two satellites originated from the accumulation in a disc of debris orbiting around the Mars that were ejected by a giant impact of a protoplanet. If so, dark, red-sloped, and featureless spectra for these satellites may be accounted for by alteration due to shock processes and/or space weathering. In addition, while Phobos possesses the red and blue units that are spectrally different in the visible and near infrared wavelengths, there is no information about the difference in composition between the two units. Furthermore, recent observations with the continuous spectral reflectance (hyperspectral) data for the Moon revealed that rocks composed of anorthosites affected by space weathering show dark, red-sloped, and featureless spectra, which may resemble D-type spectra. Therefore, it remains unknown of what kind of materials the bodies showing D-type spectra are composed.
From this point of view, we focus on the Moon, because the huge data set of the hyperspectral data obtained by the recent lunar missions allow us to examine whether and what kinds of D-type like spectra could exist on the lunar surface. In this presentation, we discuss the occurrence trends and spectral characteristics of dark materials on the lunar surface based on the data mining analysis with the hyperspectral data obtained by Spectral Profiler onboard the lunar mission SELENE/Kaguya.

Keywords: Remote Sensing, Hyperspectra, Moon, Mars, Asteroid, Kaguya/SELENE

A new method to constrain the termination ages of lunar tectonic structures

*Yuko Daket[1], Atsushi Yamaji[1], Katsushi Sato[1]

1. Graduate School of Science, Kyoto University

Mare ridges, lobate scarps, and straight rilles are representative tectonic structures on the Moon. Mare ridges are interpreted as the surface expressions of thrusts and folds. Lobate scarps and straight rilles are interpreted as tectonic structures formed by thrusts and normal faults, respectively. Their formations are thought to have resulted from the subsidence of massive mare basalt fills, which has been the most popular hypothesis of the origin of lunar tectonics since the 1970's. The subsidence should have occurred syndepositionally. Since major volcanic activities on the Moon are thought to have ceased around 3.0 Ga, tectonic activities should have ceased simultaneously. However, recently found some structures are inconsistent with the hypothesis. In order to clarify the origins of the tectonic structures on the Moon, their formation ages would be a clue, although they have been only obscurely constrained.

In this study, we developed a new technique, which was named “one-dimensional crater chronology”, to constrain the termination ages of tectonic structures quantitatively. The craters superposed on a thrust indicate that they were formed after the thrust activities ceased. Therefore, the linear number densities of the superposed craters indicate the elapsed time after the thrust activities ceased. We simulated lunar surface to derive the crater size frequency distributions of craters on linear fault traces and to derive the linear number densities of craters as a function of time. The one-dimensional crater chronology requires the linear number density of superposed craters to estimate the termination age.

We applied the newly developed technique to a mare ridge in the northwestern Imbrium region. The termination age of the formation was estimated as young as ~0.2 Ga. This young ridge formation is inconsistent with the conventional hypothesis. The global cooling of the Moon or the cooling of the PKT region are possible origins.

Keywords: Moon, Tectonics, Formation Age

3D collision simulation of sintered dust aggregates

*Masamichi Nagao[1], Satoshi Okuzumi[1], Sin-iti Sirono[2], Hidekazu Tanaka[3]

1. Tokyo Institute of Technology, 2. Nagoya University, 3. Tohoku University

Dust aggregate is an aggregate of particles formed by collision coalescence of particles, become a material for the planetesimal. In order to form a dust aggregate, it is necessary that it does not break even if aggregates collide with each other. Some 3D collision simulation to research the collision velocity for catastrophic disruption has been carried out.

However, in the 3D collision simulation, the sintering effect was not taken into account. Sintering is a phenomenon that the surface molecule of the substance moves by warming the substance at a temperature slightly lower than the melting point. When sintering proceeded, the plasticity is lost and substance becomes brittle while it becomes hard. Considering aggregate sintering, the contact surface between the particles becomes thick, and the behavior when aggregates collide with each other is also change. Currently, Aggregate collision simulation with the effect of sintering in two dimensions is already done. The result of the research shows that aggregates break at lower collision velocity when sintering occurs.

In this study, a 3D collision simulation with the effect of sintering was carried out. That purpose is to compare 2D and 3D with respect to the effect of sintering on collision of dust aggregates.

First, on the basis of the model used in the 2D collision simulation with the effect of sintering, we made the model that can be applied to three dimensions. We introduced a force that is applied when the two contacting particles twist, which is not taken into account in the 2D simulation. In this simulation, we investigated the critical velocity for catastrophic disruption and how the number of contact points changed as a result of collision.

As a result of 3D simulation, depending on the progress of sintering, the different critical velocity for catastrophic disruption was obtained. The critical velocity for catastrophic disruption of sintered aggregates is lower than it of non-sintered aggregates. Also, although the qualitative tendencies of the result are similar between 2D and 3D, there are differences such as rebound.

This study showed that sintering affected collision of dust aggregates in 3D. When sintering occurs, the aggregate that collided is easily broken like the result in 2D simulation .

From now on, we need to further study the distribution of fragment and aggregate compression.

Keywords: Sintering, Dust aggregate, Simulation

Heating inside a highly-porous dust aggregate

*Sin-iti Sirono[1]

1. Department of Earth and Planetary Sciences, Nagoya University

At the beginning of planetary formation, highly porous dust aggregates are formed. Outside the snowline, the main component of an aggregate is H_2O ice. Because H_2O ice is formed as amorphous ice, its thermal conductivity is small. Thermal conductivity of icy dust aggregate is small accordingly. Then it is possible to heat up inside an aggregate due to decay of radionuclides contained in silicate cores of dust grains. It is shown that the temperature increases substantially inside an aggregate, leading to crystallization of amorphous ice. During the crystallization, temperature further increases enough to proceed sintering. The mechanical properties of icy dust aggregates can change greatly, and collisional evolution of dust aggregate is affected by sintering. The latent heat of crystallization depends on chemical composition of ice. The maximum temperature depends on the composition accordingly. If the amount of impurities is large, heating by crystallization is suppressed.

Keywords: dust aggregate, heating, sintering

Collisional Growth and Internal Density Evolution of Icy Dust Aggregate in Disk Formation Stage

*Kenji Homma[1], Taishi Nakamoto[1]

1. Department of Earth and Planetary Sciences, Tokyo Institute of Technology

Planetesimals are building blocks of planets so it is important to investigate when and where planetesimals form in protoplanetary disks. However, there are some obstacles to form planetesimals from dust by collisional growth. One of the most serious barrier is the radial drift of macroscopic dust aggregates toward the central star due to the gas drag. On the other hand, it is suggested that highly porous dust aggregates break through the radial drift barrier. In the minimum mass solar nebula model, highly porous icy dust aggregates can grow to planetesimal-sized objects by direct collisional growth inside the disk (Okuzumi et al. 2012, Kataoka et al. 2013). However in these studies, it is not considered when the collisional growth begins in protoplanetary disks. If there is no process that suppresses collisional growth of icy dust aggregates, collisional growth may begin from the protoplanetary disk formation stage.
To investigate how the disk evolution in disk formation stage affects the collisional growth and internal density evolution of porous icy dust aggregates, we have calculated the evolution of radial size distribution of icy dust aggregates using the disk model including mass accretion from molecular cloud core developed by Nakamoto & Nakagawa (1994) and Hueso & Guillot (2005).
As a result, we find that icy aggregates cannot become highly porous as previous studies (Okuzumi et al. 2012, Kataoka et al. 2013), and they suffer the radial drift without growth to planetesimal-sized object. Because the small dust particles from molecular cloud core contribute the growth of aggregates in earlier phase of their growth, the aggregates cannot have many voids until they become large size that collisional compression works effectively. This result suggests that a process that suppresses collisional growth of icy dust aggregates in early stage of protoplanetary disks is present and the age of planetesimals would not be very young.

Dust and gas co-evolution with dust-gas backreaction in protoplanetary disks

*Takahiro Ueda[1], Kazuhiro Kanagawa[2], Takayuki Muto[3], Satoshi Okuzumi[1]

1. Department of Earth and Planetary Sciences, Tokyo Institute of Technology, 2. University of Szezecin, 3. Division of Liberal Arts, Kogakuin University

Planetesimal formation has to overcome two major barriers. The first one is the radial drift barrier. Dust particles in protoplanetary disks feel a headwind from the surrounding disk gas. Due to the gas-dust friction, dust particles lose their angular momentum and drift inward. The second one is the fragmentation barrier. The collision velocity of dust particles can be too high for the particles to stick together. Recently, Gonzalez et al. (2017) have shown in their 3D SPH simulations that the backreaction from dust to gas affects the disk gas structure so that the dust particles can overcome these barriers. In their simulations, dust particles pile up due to the fragmentation or rapid growth. This dust concentration provides a positive torque for the surrounding gas and makes the gas moving outward. The modified gas structure prevents dust particles from drifting inward. However, Gonzalez et al. (2017) have only performed simulations with large viscosity and specific disk conditions, hence how the effect of the backreaction depends on disk parameters is still unclear.
Here we present analytic expressions of gas and dust velocities in protoplanetary disks including the effect of backreaction from dust to gas. These analytic formulas allow us to describe the dust and gas co-evolution including the effect of the frictional force from dust particles. The analytic formulas suggest that the backreaction forces the gas move outward even if the dust-to-gas mass ratio is lower than the standard value of 10^{-2}, as long as the gas viscosity is small. We also present the results of 1D and 2D dust-gas two-fluid simulations to demonstrate the backreaction changes their evolution. We find that when the viscosity is small or the dust-to-gas mass ratio is high, the outward motion of the gas provides a positive surface density gradient in some part of the disk.

Keywords: protoplanetary disks

Rocky Planetesimal Formation by Gravitational Instability of a Porous Dust Disk

*Misako Tatsuuma[1,2], Shugo Michikoshi[3], Eiichiro Kokubo[2,1]

1. The University of Tokyo, 2. National Astronomical Observatory of Japan, 3. University of Tsukuba

Recently, it is proposed that porous dust aggregates are formed by pairwise accretion of silicate dust aggregates, which can avoid the radial drift and fragmentation barriers during their growth if the dust monomer size is on the order of nm [1]. Indeed, it is suggested that dust monomers in protoplanetary disks are not same as sub μm-sized interstellar dust grains, but they have experienced evaporation and condensation [1]. Moreover, matrix grains in primitive meteorites [2] and interplanetary dust particles [3] contain nm-sized grains.

We investigate the gravitational instability (GI) of the disk consisting of porous dust aggregates of nm-sized silicate monomers. We calculate the equilibrium random velocity of the dust aggregates considering gravitational scattering and collisions among them, gas drag, and turbulent stirring and scattering according to Michikoshi & Kokubo (2016) [4], and then evaluate Toomre's stability parameter Q [5]. The condition for the GI is defined as $Q < 2$ taking into account the non-axisymmetric mode [6]. We find that for the minimum mass solar nebula (MMSN) model at 1 au, the disk becomes gravitationally unstable as the dust aggregates evolve through gravitational compression if turbulent strength is $\alpha < 5\times 10^{-5}$. We also derive the critical disk mass and dust-to-gas ratio for the GI as a function of α.

References: [1] Arakawa, S., & Nakamoto, T. 2016, ApJL, 832, L19 [2] Toriumi, M. 1989, Earth and Planetary Science Letters, 92, 265 [3] Keller, L. P., & Messenger, S. 2011, GeoCoA, 75, 5336 [4] Michikoshi, S., & Kokubo, E. 2016, ApJL, 825, L28 [5] Toomre, A. 1964, ApJ, 139, 1217 [6] Toomre, A. 1981, in Structure and Evolution of Normal Galaxies, ed. S. M. Fall & D. Lynden-Bell, 111–136

Figure 1. (left) Toomre's Q in the m_d-ρ_{int} plane at 1 au for the MMSN disk with $\alpha = 10^{-5}$, where m_d is the mass and ρ_{int} is the mean internal density of the dust aggregates. The dash-dot, solid, and dash contours correspond to Q = 1, 2, and 4, respectively. The dot line shows the evolutional track of dust aggregates.

Figure 2. (right) Disk parameters for the GI at 1 au. The red triangle, blue circle, and black square shows $\alpha = 10^{-2}$, 10^{-3}, and 10^{-4}, respectively.

Keywords: planetesimal formation, protoplanetary disk, gravitational instability, porous dust aggregate

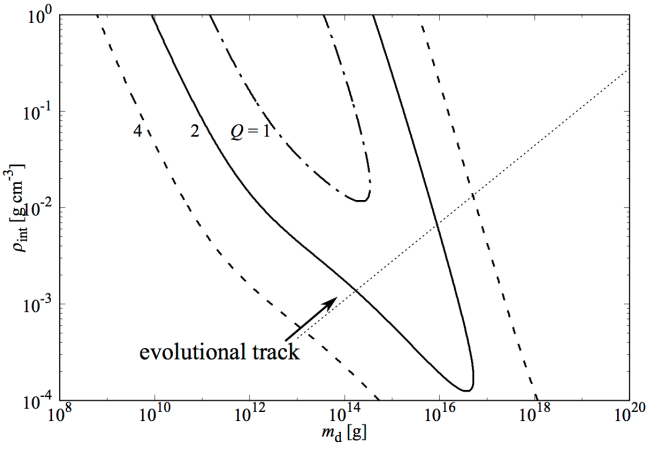

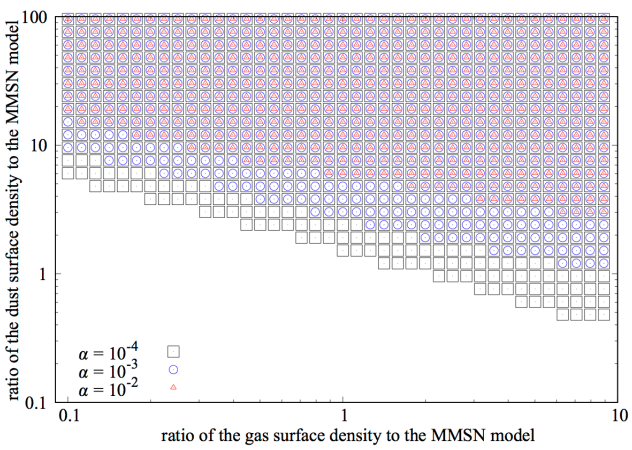

Condition of the efficient formation of dense dust clumps due to the streaming instability

*Tetsuo Taki[1], Ryo Hasegawa[2], Masaki Fujimoto[2]

1. National Astronomical Observatory of Japan, 2. Institute of Space and Astronautical Science, Japan Aerospace Exploration Agency

Planetesimal formation is the key process for the planetary system formation. There are, however, many theoretical difficulties to form planetesimals. The fragmentation barrier is one of the most serious problem for planetesimal formation (Blum & Munch, 1993). The maximum size of dust particles is limited to about millimeters to centimeters by this barrier. We need a model to connect these small dust particles or pebbles to planetesimals.

The streaming instability is one of the promising process to form planetesimals (Youdin & Goodman, 2005; Johansen et al., 2012). This instability can form the dense dust clumps consisting of millimeter- or centimeter-sized particles. These dense dust clumps are sometimes gravitationally bound and are considered to form planetesimals by subsequently self-gravitational collapse.

Whether the streaming instability can form dense dust clumps depends on the particle size and the dust-to-gas ratio of protoplanetary disks. Carrera et al. (2015) conducted a parameter survey to find the critical dust-to-gas ratio for strong clumping due to the streaming instability at each particle size.

In this study, we focus on the efficiency of the formation of dense dust clumps. We conducted 2D simulations of dust-gas system like Carrera et al. (2015). We investigated how much dust particles contribute to clumping in the parameter space where indicated as being appropriate for formation of dense dust clumps by Carrera et al. (2015). Then we compared the mass of the entire dust particles that contributed to clumping with the mass of solar system planets, looking for conditions suitable for solar system formation. We found that a sufficient amount of particles contribute to clumping when dust-to-gas ratio is 0.04 even though the dust particles have relatively small radius about 1 mm.

Keywords: Protoplanetary disk, Planetesimal formation, Planetary system formation

Co-Accretion of Chondrules and Fluffy Matrices

*Sota ARAKAWA[1], Taishi Nakamoto[1]

1. Tokyo institute of technology

Chondrules are the principal components of the most common meteorites, chondrites. This facts may mean that rocky planetesimals in our solar system are formed via accretion of chondrules. However, it is not yet understood how chondrules grow into planetesimals.
Several pieces of meteoritical evidence suggest that chondrites contained abundant nanograins in their matrices. These nanograins must play a key role for growth of dust aggregates. Therefore we examined a scenario in which rocky pkanetesimals are formed via co-accretion of chondrules and fluffy aggregates of nanograins.
Though our scenario succeeded in forming rocky planetesimals, we also found a new problem for "chondritic" planetesimal formation. If the mass fraction of chondrules is not hight enough, and the density of matrices is too low to stop chondules when dust aggregates collide, then the retainment of chondrules in fluffy matrices is nontrivial. Future work on this point is needed.

Keywords: Rocky planetesimal, Chondrule

Effects of magnetically-driven disk winds on type I migration

*Masahiro Ogihara[1], Eiichiro Kokubo[1], Takeru Suzuki[2], Alessandro Morbidelli[3], Aurélien Crida[3]

1. National Astronomical Observatory of Japan, 2. University of Tokyo, 3. Observatoire de la Cote d'Azur

Magnetically-driven disk winds would alter the surface density slope of gas in the inner region of a protoplanetary disk ($r < 1$au), which in turn affects migration of low-mass planets (type I migration). Recently, the effect of disk wind torque has been considered, showing that it would carve out the surface density of the disk from the inside out.

The direction and rate of type I migration depend on the surface density slope of gas and saturation of the corotation torque. We investigate migration of low-mass planets in disks evolving via disk winds. In MRI-active disks, the surface density slope can be flat in the inner region, and migration of super-Earth mass planets is suppressed. In MRI-inactive disks, in which a positive surface density slope can be achieved, planets in the sub-Earth mass range may undergo outward migration.

It has also been pointed out that the wind torque induces global gas flows (wind-driven accretion), which may modify the desaturation effect of the corotation torque. Then, we investigate effects of wind-driven accretion (global gas flows) on type I migration. In MRI-inactive disks, in which the wind-driven accretion dominates the disk evolution, the gas flow at the midplane plays an important role. If this flow is large, the corotation torque is efficiently desaturated. Then, the fact that the surface density slope can be positive in inner region due to the wind torque can generate an outward migration region extended to super-Earth mass planets. In this case, we observe that no planets fall onto the central star in *N*-body simulations with migration forces imposed to reproduce such migration pattern.

Keywords: Magnetically-driven disk winds, Type I migration, Protoplanetary disk, N-body simulation

Satellite formation via pebble accretion in circumplanetary disks

*Yuhito Shibaike[1], Satoshi Okuzumi[1], Takanori Sasaki[2], Shigeru Ida[3]

1. Department of Earth and Planetary Sciences, Tokyo Institute of Technology, 2. Department of Astronomy, Kyoto University, 3. Earth-Life Science Institute, Tokyo Institute of Technology

The four icy satellites around Jupiter called "Galilean satellites" are considered to have formed in a circumplanetary disk. In Shibaike et al. in prep., we calculated the growth and drift of dust particles in a steady circumplanetary disk and investigated the success condition of satellitesimal formation. We found that the dust-to-gas inflow mass flux ratio has to be higher than unity for the satellitesimal formation in the circumplanetary disk by the collisional growth of the dust particles and that the all dust particles drift to Jupiter in other conditions. However, it is difficult to achieve this success condition.
Recently, a new planetary formation model called "pebble accretion" has been attracted attention. In this model, several protoplanets accrete a lot of cm-sized dust particles (called "pebbles") drifted from the outer region of the protoplanetary disk and grow rapidly to planets.
In this work, we applied this "pebble accretion" model to satellite formation. We calculated the growths of the protosatellites accreting the dust particles growing and drifting in the circumplanetary disk. Figure 1 represents the growths of the protosatellites on the fore fixed current Galilean satellites' orbits when the gas inflow mass flux is $0.14 M_J/\mathrm{Myr}$ and the strength of turbulence in the viscous accretion disk is $\alpha=10^{-4}$. We found that there is a possibility that the protosatellites can grow to the planets with the mass of the Galilean satellites, 10^{23} kg, within 10^5-10^7 years even in the case with that the dust-to-gas mass inflow flux ratio is 0.01. Figure 2 represents the timescales of the growths of the protosatellites and the inward drifts by Type I migration. Our estimate suggested that the protosatellites drift to Jupiter by the Type I migration because the growth timescales become longer than the drift timescales when their mass reach 10^{21} kg. We used a simple model assuming steady states in these estimates. We will discuss the satellite formation in unsteady states, in other words, the evolutions of the circumplanetary disk and the orbits of the protoplanets in our talk.

Keywords: Satellite, Pebble accretion, Protosatellite, Circumplanetary disk, Galilean satellites, Type I migration

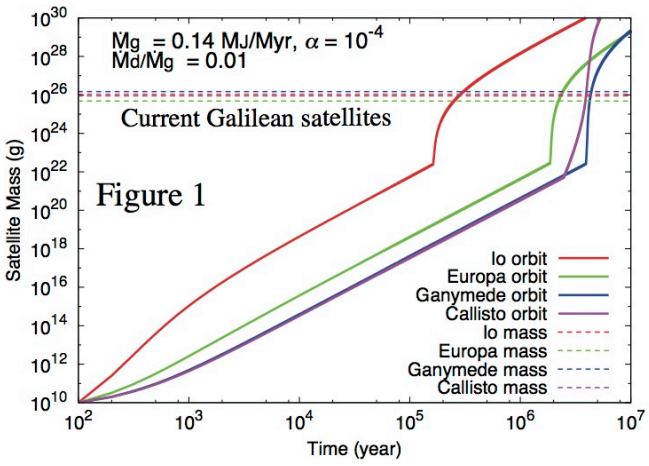

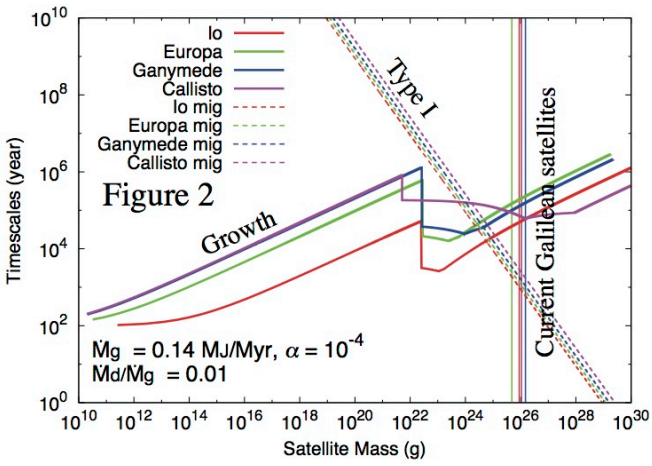

Terrestrial magma ocean origin of the Moon: A numerical study of a giant impact incorporating the difference of the equations of state for liquids and solids

*Natsuki Hosono[1,2], Shun-ichiro Karato[3], Junichiro Makino[4,2,5]

1. Kyoto University, 2. AICS, RIKEN, 3. Yale University, 4. Kobe University, 5. Tokyo Institute of Technology

The origin of the Moon is one of the most important topics in the planetary science and geophysics.
Since the giant impact (GI) scenario was suggested, it has been believed that the Moon was formed by the impact of relatively large object (Mars-size) to a growing Earth.
Recently, however, the GI has been challenged; the isotope ratios of particular elements show nearly identical values for the bulk component of the Earth and that of the Moon.
This means that the Moon should have been formed from the proto-Earth originated materials.
However, previous numerical simulations of the GI concluded that the Moon was formed from the impactor.
In order to resolve this problem, several modified models to the GI have been suggested.
However, most of them have difficulties to explain much higher angular momentum and the dissimilarity of the FeO content.
Recently, a new model, to form the Moon from the Earth’s magma ocean, is suggested.
According to this scenario, the majority of heating occurs in the terrestrial magma ocean, which results in the ejection of the target-originated materials.
Since the formation of the FeO-rich magma ocean is a natural consequence of the formation of the proto-Earth, this scenario can also explain the dissimilarity of the FeO content.
We carried out the numerical simulations of GI in which the magma ocean is modeled with an equation of state for liquid.
We show the comparisons of the GI between liquid equation state and solid one.

Collisional fragmentation of planetesimals in the giant impact stage

*Hiroshi Kobayashi[1], Yutaro Sato[1]

1. Department of Physics, Nagoya University

Mars-sized protoplanets formed in a protoplanetary disk further grow to be terrestrial planets via mutual collisions between protoplanets or "giant impacts" after gas depletion, which are believed to from the terrestrial planets in the solar system. The resultant planets mainly have eccentricities much larger than those of Earth and Venus, so that the dynamical friction of a planetesimal disk is needed for eccentricity damping. However, planetesimals stirred by planets are dynamically so hot that collisional fragmentation of planetesimals inhibits the dynamical friction. Therefore, the N-body simulation including collisional fragmentation as well as dynamical friction is required for the investigation of giant impact stage. We newly develop the N-body code with protoplanets and super particles representing planetesimals and smaller fragments. Through the simulations with the code, we give constrains on the total mass and radii of planetesimals remaining in the giant impact stage.

Keywords: Planet formation, collisional fragmentation

Terrestrial Planet Formation: Constraining the Formation of Mercury

*Patryk Sofia Lykawka[1], Takashi Ito[2]

1. Astronomy Group, School of Interdisciplinary Social and Human Sciences, Kindai University, 2. National Astronomical Observatory of Japan

The formation of Mercury remains poorly understood. Importantly, previous works have not considered the formation of Mercury in the context of formation of the other terrestrial planets.

We investigated terrestrial planet formation by performing N-body simulation runs using hundreds of embryos and thousands of disk planetesimals representing a primordial protoplanetary disk. To investigate the formation of Mercury, these simulations considered an inner region of the disk (the Mercury region) and disks with and without mass enhancements beyond the ice line location in the disk.

Although Venus and Earth analogs (considering both orbits and masses) successfully formed in the majority of the runs, Mercury analogs were obtained in lesser runs. Our Mercury analogs concentrated at orbits with semimajor axes slightly smaller than that of Mercury (a = 0.39 au), relatively small eccentricities/inclinations, and median mass m ~ 0.2 Earth masses with variations within a factor of a few. In addition, we found that our Mercury analogs acquired most of their final masses from embryos/planetesimals initially located between the disk inner edge and ~1–1.5 au within 10 Myr, while the remaining mass came from a wider region up to ~3 au at later times. These results suggest that to reproduce the orbit and mass of Mercury, the protoplanetary disk should have an inner edge at a 0.3 au with mass peak located beyond 0.6 au. Also, the Mercury region should be mass depleted.

Keywords: planet formation, inner solar system, terrestrial planets, Mercury, solar system

Re-analysis of images of GANYMEDE

*Naoyuki Hirata[1]

1. Kobe University

Ganymede is one of Jupiter’ s moons. Numerous images of its surface have been obtained by the Voyager and Galileo spacecraft, which allow us to investigate the global distributions of dark/bright terrains or impact craters exceeding 20km in diameter. However, most of Ganymede is imaged at a resolution of 1km/pixel or higher, and therefore, we can hardly examine the global distribution of smaller features of Ganymede. I re-analyses the Voyager and Galileo images, using multi-flame image restoration.

Keywords: GANYMEDE

Atmospheric Evolution of the Terrestrial Planets during the Heavy Bombardment: the Effects of the Element Partitioning

*Sakuraba Haruka[1], Hiroyuki Kurokawa[2]

1. Tokyo Institute of Technology, 2. Earth-Life Science Institute

The atmospheres on terrestrial planets are believed to be formed as a consequence of the impact degassing and erosion of volatiles during the Heavy Bombardment Period. Despite their common origin, there are distinct gaps in the noble gas abundances in the atmospheres on Venus, Earth, and Mars; compared to Earth, Venus is enriched and Mars is depleted in noble gases roughly by two orders of magnitude, respectively. The origin of these gaps has been poorly understood.

A possible mechanism to create these gaps is the partitioning of elements in the different surfacial environments: the runaway greenhouse on Venus, the carbon cycle on Earth, and the CO_2-ice formation on Mars. Although noble gases are mainly partitioned into the atmosphere, the distinct environments on the three planets create the differences in the noble gas concentrations in their atmospheres, leading the differences in the escape rates of noble gases due to the impact erosion.

We calculated the evolution of early atmospheres during the Heavy Bombardment Period by solving deterministic differential equations. Atmospheric components are, H_2O, CO_2, N_2, and noble gases. Because the abundances of noble gases are small, we treated both N_2 and noble gases as a component N_2 in our numerical model. The new idea of this work is to consider the partitioning of elements between atmosphere and other reservoirs. Whereas all volatiles are partitioned into atmosphere on Venus, H_2O and CO_2 are partitioned into oceans and carbonates on Earth and into ice on Mars. We set the upper limits of the partial pressures of H_2O and CO_2 considering the phase equilibrium and the steady state of the carbon cycle. Impact erosion of atmospheres and impactors are taken into account by using models of Svetsov (2000) and Shuvalov (2009). We assumed carbonaceous chondrites from the main asteroid belt as impactors. Total masses of impactors correspond to 1% of the planetary masses.

We found that the resulting abundances of N_2 and noble gases differ only by ~10% among the three planets. This is caused by the dominance of the replenishment of atmophiles over the erosion. The small differences in the abundances were due to the differences in the surface temperature and in the size of planets. The partitioning of elements was found to be less important for the abundances of N_2 and noble gases in the assumed conditions, where the delivery of atmophiles dominates. We also investigated the dependences on the impact erosion models, impactor size distributions, and types of impactors. Based on the results, we discuss the implications for the origins of volatiles and early planetary environments at ~4 Ga.

Keywords: Heavy Bombardment Period, impact erosion, noble gases

Effects of hydrogen on thermal evolution of magma ocean and early surface environment

*Keiko Hamano[1], Hidenori Genda[1], Yutaka Abe[2]

1. Earth-Life Science Institute (ELSI), Tokyo Institute of Technology, 2. Department of Earth and Planetary Science, The University of Tokyo

The standard model of planet formation suggests that terrestrial planets would experience global melting due to giant impacts, i.e. the formation of a magma ocean. Early atmosphere would form through degassing from the interior, and its greenhouse and blanketing effects would be essential to radiative heat balance at the planetary surface, limiting heat flux from the magma ocean.
Recently, several groups have been working on a coupled evolution of early atmosphere and magma ocean, and have investigated the thermal history and volatile budgets on early terrestrial planets(e.g. Elkins-Tanton 2008, Hamano et al. 2013,2015, Lebrun et al. 2013). They have focused on oxidizing atmospheres consisting of water and carbon dioxide, while early atmosphere might have reducing gaseous species. Hydrogen molecule is one of the candidates, since planets could capture nebula gas during formation or it could be produced by chemical reaction between water and metallic iron that could be scattered on giant impact events. In this talk, we would like to discuss contributions of hydrogen on early evolution of terrestrial planets.

Keywords: Magma ocean, Reducing atmospheres, Formation of oceans, early climate and surface environment

LOW-CO_2 ATMOSPHERE ON EARLY MARS INFERRED FROM MANGANESE OXIDATION EXPERIMENTS.

*Shoko Imamura[1], Natsumi Noda[1], Yasuhito Sekine[1], Soichiro Uesugi[1], Minako Kurisu[1], Chihiro Miyamoto[1], Haruhisa Tabata[1], Takashi Murakami[1], Yoshio Takahashi[1]

1. University of Tokyo

Introduction

Both CO_2 and O_2 are important atmospheric components for climate and chemical evolution on early Mars. Several lines of geological and geomorphological evidence show that early Mars has been once warm sufficient to hold liquid water on the surface at least episodically in the late Noachian and early Hesperian [1]. Although early Mars would not be warmed sufficiently by CO_2 alone, climate models presume the presence of a thick CO_2 atmosphere to decrease outgoing longwave radiation and to cause effective collision-induced absorption. However, pCO_2 on early Mars is poorly constrained by geochemical evidence thus far. On the other hand, the Curiosity rover has discovered Mn oxides in fracture-filling materials in sandstones of the Kimberley region of the Gale crater [2]. Given pO_2 capable for deposition of Mn oxides (pO_2 > ~0.01 bar) [3], the findings of Mn oxides indicate that early Mars had a substantial O_2 in the atmosphere.

The present study aims to further constrain the composition of early Mars' atmosphere, especially the CO_2/O_2 mixing ratio, at the time when the Mn oxides were formed. We performed laboratory experiments to generate Mn precipitates from Mn^{2+} in solutions by introducing CO_2/O_2 gas mixtures. We investigated the compositions of Mn precipitates under various compositions of CO_2/O_2.

Materials & Methods

The Mn^{2+} starting solution with 20 mM and pH 8–9 was prepared in an Ar-purged glovebox, where pO_2 remained < 10^{-12} bar. The starting solution was deaerated by pure Ar gas for more than 6 hours prior to the use. Then, we introduced gas mixtures of pure CO_2 and artificial air (N_2/O_2 = 4; pCO_2 < 1ppm) into the starting solution at four different mixing ratios (CO_2/O_2 = 2, 0.2, 0.02, and artificial air) in the glovebox. Note that MnO_2 is thermochemically stable under all of these conditions. Solution samples were collected in several times during the experiments. The samples were filtered through a membrane with pore size of 220 nm. After the reactions, Mn precipitates were collected by filtering the rest of the solutions using a membrane with 220 nm. Mn^{2+} concentrations of the filtered solution samples were measured using inductively-coupled plasma atomic emission spectroscopy (ICP-AES). The collected Mn precipitates were analyzed with X-ray absorption fine structure (XAFS) and X-ray diffraction (XRD).

Results

Our results of the ICP-AES analysis show that Mn^{2+} concentrations in the filtered solutions decrease over reaction time, which indicate that a part of dissolved Mn^{2+} was converted into solid precipitates. Despite both the wide range in CO_2/O_2 ratios and thermochemical stability of MnO_2 under the experimental conditions, the results of XAFS analyses show that all of the Mn solid precipitates formed under these conditions are mainly composed of Mn carbonate, namely $MnCO_3$. These results are consistent with our XRD results. Our results show that $MnCO_3$ precipitated before the formation of MnO_2 even very low CO_2/O_2 of 0.02. This suggests that kinetics of formation of $MnCO_3$ and Mn oxides are the critical factor. On the other hand, the major peaks of the XANES spectra for the collected solid precipitates at CO_2/O_2 = 0 (namely, pure artificial air) would be a mixture of Mn oxides and $Mn(OH)_2$.

Discussion

Our results show that, in order to form MnO_2 in Mn^{2+} solutions by reactions with CO_2/O_2 gas mixtures, the CO_2/O_2 ratio should be lower than 0.02. Assuming pO_2 of ~0.01–0.2 bar, which is capable to form and preserve MnO_2 in sediments [3], the observations of both a lack of $MnCO_3$ and presence of MnO_2 in Gale infer that pCO_2 on early Mars would have been less than 0.004 bar, or 4 mbar. This implies that early Mars may have possessed a low-CO_2 and high-O_2 atmosphere.

[1] Ehlmann, B.L. et al. (2011). *Nature* 479, doi:10.1038/nature10582.
[2] Lanza, N.L. et al. (2016). *Geophys. Res. Lett.*, 43, 7398-7407.
[3] Shaw, T. et al. (1990). *Geochim. Cosmochim, Acta 54,* 1233-1246.

Keywords: Mars, planetary evolution, atmospheric composition

Superflares on G-, K-, M- type stars

*Yuta Notsu[1], Hiroyuki Maehara[2], Namekata Kosuke[1], Shota Notsu[1], Kai Ikuta[1], Satoshi Honda[3], Daisaku Nogami[1], Kazunari Shibata[4]

1. Department of Astronomy, Graduate School of Science, Kyoto University, 2. Okayama Astrophysical Observatory, NAOJ, 3. Center for Astronomy, University of Hyogo, 4. Kwasan and Hida Observatories, Graduate School of Science, Kyoto University

Flares on G, K, M-type stars are sudden releases of the magnetic energy stored around the starspots, like solar flares. Recent high-precision photometry from space shows that "superflares", which are 10-10^4 times more energetic than the largest solar flares, occur on many G, K, M-type stars including Sun-like stars (slowly-rotating G-type main-sequence stars like the Sun) (e.g., Maehara et al. 2012 Nature). Such superflares emit harmful UV/X-ray radiation and high-energy particles such as protons, and may suggest that exoplanet host stars have severe effects on the physical and chemical evolution of exoplanetary atmospheres (cf. Segura et al. 2010 Astrobiology, Takahashi et al. 2016 ApJL). It is then important to know the detailed properties of such superflare events for considering the habitability of planets.

In this presentation, we present statistical properties of superflares on G, K, M-type stars on the basis of our analyses of Kepler photometric data (cf. Maehara et al. 2012 Nature, Shibayama et al. 2013 ApJS, Notsu et al. 2013 ApJ, Maehara et al. 2015 EPS). We found more than 5000 superflares on 800 G, K, M-type main-sequence stars, and the occurrence frequency (dN/dE) of superflares as a function of flare energy (E) shows the power-law distribution with the power-law index of -1.8~-1.9. This power-law distribution is consistent with that of solar flares.
Flare frequency increases as stellar temperature decreases. As for M-type stars, energy of the largest flares is smaller (~10^{35} erg) compared with G,K-type stars, but more frequent "hazardous" flares for the habitable planets since the habitable zone around M-type stars is much smaller compared with G, K-types stars.

Flare frequency has a correlation with rotation period, and this suggests young rapidly-rotating stars (like "young Sun") have more severe impacts of flares on the planetary atmosphere (cf. Airapetian et al. 2016 Nature Geoscience). Maximum energy of flares and flare frequency also depends on the area of starspots, and this suggest existence of large starspots is important factor of superflares.
The statistical properties of superflares discussed here can be one of the basic information for considering the impacts of flares on planet-host stars.

Keywords: flare, Kepler, habitability

The effect of spectral type of central star on climate and climatic evolution of the Earth-like planets in habitable zone

*Shintaro Kadoya[1], Eiichi Tajika[1]

1. Department of Earth and Planetary Science, Graduate School of Science, The University of Tokyo

The climate of the Earth depends on both insolation and the amount of greenhouse gases, especially CO_2, in the atmosphere. Owing to a negative feedback mechanism in carbonate-silicate geochemical cycle system (so called the "Walker feedback"), the amount of CO_2 in the atmosphere (pCO_2) is regulated so that the climate of the Earth may be warm (i.e., the climate is warm enough for liquid water to exist on the surface of the Earth). However, if the CO_2 degassing rate via volcanic activities is below some critical value, the Walker feedback mechanism cannot maintain a sufficient amount of CO_2, and the Earth becomes globally ice-covered. Here, the critical value of the CO_2 degassing rate is a critical condition under which the Earth becomes globally ice-covered owing to a large ice-cap instability. Since albedo of ice depends on the spectrum of the insolation, the critical condition for the Earth to be globally ice-covered is expected to be different from previous estimates when the central star is different from the Sun. The difference in the spectral type of the central star due to different mass also results in different evolutionary timescale of its luminosity which affects the habitable zone (HZ) around it. In this study, we examine the climate and the climatic evolution of the Earth-like planets around different-mass stars.
We use a one-dimensional energy balance model coupled with a carbon cycle model to estimate the climate, and the planetary albedo model is improved in order to examine the effect of the difference in the spectrum of the insolation from the central star. The evolution of the climate is examined based on the evolutions of CO_2 degassing rate and insolation, which are estimated by a parameterized convection model coupled with a mantle degassing model and a luminosity evolution model, respectively. Four types of stars (i.e., M-, K-, G-, and F-type stars) are considered.
Comparing stars with different mass (e.g., M- and G-type stars), pCO_2 of an Earth-like planet around a light star (i.e., the M-type star) tends to be lower than that of an Earth-like planet around a heavy star (i.e., G-type star) for the same luminosity and CO_2 degassing rate. This is because the peak wavelength of the insolation of the light star is longer than that of the heavy star, and because the ice absorbs longer-wavelength radiation more than shorter-wavelength radiation. As a result, the critical CO_2 degassing rate is less in the inner region of the HZ around the light star than in the region around the heavy star. However, when the Earth-planet is in the outer region of the HZ, and pCO_2 is high owing to the Walker feedback, the critical CO_2 degassing rate of the Earth around the light star is almost the same as that of the Earth around the heavy star especially in the outer region of the HZ because the surface albedo does not affect the planetary albedo owing to the dense atmosphere. Thus, regardless of the spectral type of the central star, the timescale for the warm climate of Earth-like planet is about 4 billion years which depends, not on the insolation, but strongly on the evolution of the CO_2 degassing rate of the planet. These results indicate that we should search for the inner region of the HZ around young stars to find Earth-like habitable planets.

Keywords: Exoplanet, Carbonate-silicate geochemical cycle, Habitable planet

Modeling Dust Cloud Structure in Super-Earth GJ1214b: Implications for the Atmospheric Metallicity

*Kazumasa Ohno[1], Satoshi Okuzumi[1]

1. Department of Earth and Planetary Science, Tokyo Institute of Technology

Recent transit observations have revealed that many exoplanets have featureless spectra. Such spectra indicate extremely metal-enhanced atmospheres or the presence of opaque clouds at high altitude. Although thick high-altitude clouds prevent us from directly probing the atmosphere beneath them, their existence might provide us some information about the dynamics and/or composition of the lower atmosphere. However, it is still unclear how atmospheric dynamics and composition would affect cloud structure in exoplanets because most previous studies neglected or at least parameterized the growth microphysics of condensate particles.

In this study, we aim to understand the relationship between the atmospheric metallicity and the vertical extent of dust clouds. Recently, we have developed a new cloud model that takes into account the vertical transport of condensate particles and particle growth via both condensation and coalescence (Ohno & Okuzumi 2017). With our cloud model, we examine the vertical distributions of dust clouds in GJ1214b as a function of atmospheric metallicity.

We find that the cloud top reaches beyond 10^{-3} bar for atmospheric metallicities of 10× solar abundance, but does not reach the height of 10^{-5} bar for all choices of the model parameters. From timescale arguments, we find that the dust cloud structure can be classified into three regimes: *Condensation–Diffusion* regime, *Coagulation– Diffusion* regime, and *Coalescence–Sedimentation* regime. The maximum height of the cloud top occurs at the transition of the *Coagulation–Diffusion* and *Coalescence–Diffusion* regimes. Comparison between the maximum height of the cloud top predicted from our model and the height indicated from the observations of GJ1214b rules out atmospheric metallicities of 1–100× solar abundance for this particular exoplanets. Consequently, our results suggest that the atmosphere of GJ1214b is depleted in hydrogen as suggested by previous independent modeling, or the cloud in GJ1214b is composed of haze particles produced by photochemical reactions at high altitude.

Keywords: super-Earth, Dust Clouds, Atmospheric Metallicity

The structure of mantle convection in super-Earths of various sizes

*Takehiro Miyagoshi[1], Masanori Kameyama[2], Masaki Ogawa[3]

1. Japan Agency for Marine-Earth Science and Technology, 2. Ehime University, 3. University of Tokyo

The structure of convection in the mantle of super-Earths is one of the most important issues in studies of their thermal history and surface environment which is linked to the habitability of planets. In our past studies (Miyagoshi et al., 2014 ApJL, 2015 JGR), we showed that the effects of strong adiabatic compression substantially reduces the activity of hot ascending plumes and the efficiency of convective heat transport in massive super-Earths(about ten times the Earth’ s mass).
In this paper, we show that how convective structure changes as the mass of the planet increases. In the Earth-like size planet, hot plume activity is high, but the activity is reduced as the planet mass increases. When Mp (the planet mass divided by the Earth’ s mass) exceeds 4, hot plumes become faint compared with cold ones and their activity becomes negligible. The dimensional thickness of the lithosphere increases as Mp increases in spite of the increasing Rayleigh number. The rms velocity of thermal convection does not significantly depend on Mp. These results suggest that plate tectonics becomes harder to operate as Mp increases.
We also explored the initial transient stage of thermal convection in massive super-Earths. When the shallow mantle is initially hotter than expected from the adiabatic extrapolation from the deep mantle, as expected when the planet is formed from giant impact, transient layered convection continues for as long as several to ten billion years before it yields to a whole layer convection that occurs as the structure in the statistically steady state. Our results suggest that the interior of many of massive super-Earths may be still in the transient stage rather than the steady state now.

Keywords: super-Earths, mantle convection

An improvement of a 1D thermal evolution calculation scheme based on mixing length theory

*Shunichi Kamata[1]

1. Creative Research Institution, Hokkaido University

Solid-state thermal convection plays a major role in the thermal evolution of solid planetary bodies. Solving the equation system for thermal evolution considering convection requires a 2-D or 3-D modeling, resulting in large calculation costs. A 1-D calculation scheme based on mixing length theory (MLT) requires a much lower calculation cost and is suitable for parameter studies. A major concern for the MLT scheme is its accuracy because of a lack of detailed comparisons with higher dimensional schemes. In this study, I quantify its accuracy by comparing steady-state thermal profiles obtained by 1-D MLT and 3-D numerical schemes for different curvatures, different Rayleigh numbers, and different viscosity contrasts. For isoviscous cases, I find that relative errors for the mean temperature and Nusselt number can be up to >100% and ~50%. In order to improve the accuracy, I propose a new definition of the mixing length, which is a parameter controlling the efficiency of heat transportation due to convection. I find that the use of a smaller peak depth and a larger peak value of the mixing lengths decreases errors. I provide empirical quadratic functions for the peak depth and the peak value leading accurate results. Similar analyses were done for temperature-dependent viscosity cases. I find that the use of the new definition of the mixing length also improves results for time-dependent calculations, indicating that this approach is useful for thermal evolution studies.

Keywords: thermal evolution, numerical calculation

Viscous heating in shock-comminuted rocks: A reappraisal of the shock melting threshold by using a shock physics code

*Kosuke Kurosawa[1], Hidenori Genda[2]

1. Planetary Exploration Research Center, Chiba Institute of Technology, 2. Earth Life Science Institute, Tokyo Institute of Technology

Impact melts are among the most curious geologic samples because they provide clear evidence of hypervelocity collisions between two planetary bodies at several km/s. Thus, the required shock pressure for incipient melting after pressure release has been studied extensively. It is widely assumed that pressure release is an isentropic process. This assumption is expected to be valid when the shocked matter behaves as a perfect fluid. Since the archived shock pressure under typical collisions between two planetary bodies is thought to be much larger than the Hugoniot Elastic limit, the yield strengths of both intact and comminuted rocks have been neglected in a lot of cases. In this study, we focused on collisions at relatively low velocities, which are that the effects of the material strength cannot be neglected. The effects of internal friction in comminuted rocks, i.e., the yield strength of shock-comminuted rocks, on thermodynamic behavior on an entropy-pressure plane were investigated using the iSALE shock physics code to revisit the threshold of incipient melting against the peak shock pressure. We will present a preliminary result obtained through the numerical experiments at the meeting.
A vertical impact of a sphere onto a flat target are numerical modeled in a two-dimensional cylindrical coordinate. The analytical equation of state (ANEOS) for dunite were used for both projectile and target. Impact velocity was fixed at 6 km/s, which is slightly lower than the bulk sound velocity of dunite. The projectile radius was divided into 50 cells, which is thought to be large enough to investigate the shock pressure distribution with a high accuracy. We assumed that the projectile and the target have any temperature gradients at initial. The initial temperature was set to 220 K, which is close to a radiative-equilibrium temperature at the main belt region. The constitutive model for dunite parameterized in Johnson et al. (2015) was also used with the same input parameters except for the coefficient of internal friction. Lagrangian tracer particles were inserted into each computational cell. We stored the time variation of pressure and entropy into the tracers.
We found that the entropy gradually increases during pressure release in the case of a highly-frictional target contrary to the assumption of isentropic release. A larger value of the internal friction leads to a larger increase of entropy. We also found that the shock melting occurs after ~40 GPa shock compression under our experimental conditions if we used a typical value for the coefficient of the internal friction. This value is lower than a widely-used threshold for shock-induced melting. Our results suggest that (1) the shock melting occurs at a lower impact velocity than previously thought and that (2) the input parameters of the constitutive model in numerical models largely affect the thermodynamic response of geologic materials.

Acknowledgement: We appreciate the developers of iSALE, including G. Collins, K. Wünnemann, B. Ivanov, J. Melosh, and D. Elbeshausen.

Keywords: Hypervelocity collisions, Impact melts, Numerical modeling of impact phenomena

Efficiency of material separation caused by magnetic field in outer space recognized for solid particles in general

*Chiaki Uyeda[1], Kentaro Terada[1], Keiji Hisayoshi[1]

1. Institute of earth and Space Science Graduate School of Science Osaka University

Magnetic field gradient and dust particles coexist in various regions of galactic space. Although the field intensity in these regions are considerably low compared to the experimental conditions available on earth, the immersive microgravity duration in these area may cause specific motion of solid particles, and the translation may cause material fractionation that are observed in these regions. Magnetic separation is generally caused by a magnetic potential induced in the solid particle, and was conventionally used to collect ferromagnetic, ferrimagnetic or strongly paramagnetic materials. Whereas, it was believed that most of the existing material (i.e. diamagnetic & paramagnetic material) required ultra-strong field intensity above 10 Tesla. Field-induced translation was recently observed for single diamagnetic particles released in an area of a monotonically decreasing field, and values diamagnetic susceptibility per unit mass was detected from a small sample;[1][2] in these experiments, the grain was allowed to translate freely in a diffuse area using microgravity conditions. Based on the same principle, we found that ensembles of heterogeneous particles are separated into fractions using a neodymium hand magnet (*go to* YouTube" Magnetic separation of general solid particles realized by a permanent magnet" *for the movie*) [3] .The ensemble consisted of diamagnetic bismuth, diamond and graphite particles, as well as two paramagnetic olivine.

The setup to observe the separation was installed in a wooden box that was attached to the top position of a drop shaft (length ~1.5 m). The duration of the microgravity condition was approximately 0.5 s. With the beginning of microgravity, the a carbon sample stage inside the stage-holder was levitated, which was effective in releasing the grains in a diffuse area; here the stage was spontaneously levitated by a small field gradient applied in the vertical direction. In previous studies, it was technically difficult to release a substance in a diffuse area in μg conditions. The separation of weak magnetic material was realized because the terminal velocity of the particles that translated in an area of B=0 was uniquely determined by the intrinsic susceptibility of the material and also by the field intensity at the initial sample position; the velocity was independent to mass of particle. This relationship was directly deduced from an energy conservation rule. The result achieved here is against the generally accepted notion that ordinary solid materials (i.e. diamagnetic and paramagnetic materials) are magnetically inert. In the diffuse conditions of outer space , the effectiveness of the field-induced separation would be more efficient because the effects of viscous drag, friction and gravity are negligible. Recently the mass independent property of magnetic translation was also confirmed for ferromagnetic and ferri-magnetic grains, namely in iron, nickel and ferrite. This means that proposed principle of material separation is confirmed for all categories of magnetic materials.

References

[1] K. Hisayoshi, S. Kanou and C. Uyeda : Phys.:Conf. Ser., 156 (2009) 012021.
[2] C. Uyeda, K. Hisayoshi, and S. Kanou : Jpn. Phys. Soc. Jpn. 79 (2010) 064709.
[3] K. Hisayoshi, C. Uyeda and K. Terada : Sci. Rep. (Nature Pub) 6 (2016) 38431

Keywords: material separation, field gradient, diamagnetic anisotropy, paramagnetic anisotropy

Cratering experiments with spherical targets: The curvature effects on the cratering efficiency

*Ayako I Suzuki[1], Chisato Okamoto[2], Kosuke Kurosawa[3], Toshihiko Kadono[4], Sunao Hasegawa[1], Takayuki Hirai[5]

1. Institute of Space and Astronautical Science, Japan Aerospace Exploration Agency, 2. Graduate School of Science, Kobe University, 3. Planetary Exploration Research Center, Chiba Institute of Technology, 4. University of Occupational and Environmental Health, 5. Research and Development Directorate, Japan Aerospace Exploration Agency

Recent planetary explorations revealed that the surfaces of small bodies are covered by a large number of craters. Impact cratering processes on small bodies are expected to be largely different from those on terrestrial planets mainly because of the following two reasons. The first one is their relatively-low surface gravity. The local material strength rather than gravity is subject to control the crater size on small bodies. All the craters on the asteroids smaller than a few km in diameter are possible to be in the strength-controlled regime (Jutzi et al., 2015). Another reason is the target curvature. Thus, the understanding of the cratering processes on curved surfaces in the strength-controlled regime is essential to investigate the collision environment of small bodies through their histories.
The curvature effects on the cratering processes, such as the cratering efficiency, have not been investigated systematically, although Fujiwara et al. (1993, 2014) have produced distinctive-shaped impact craters mainly on cylindrical targets with a wide range of its radius in a laboratory, and reported the crater diameter/depth/mass increase with and the target curvature. In this study, we performed a series of impact experiments using spherical targets with different diameters. The three-dimensional topography of the produced craters on the spherical surfaces were measured in 0.2 mm/pixel, allowing us to investigate the crater dimensions as a function of the target curvature. Then, we constructed a simple model to describe the effects of target geometry on the increase of the crater radius.
Impact experiments were performed by using a two-stage light-gas gun at the facility of ISAS/JAXA. The gypsum targets were cubes with 9 cm and 15 cm on a side, and spheres with 7.8 cm, 10.9 cm, 17.0 cm, and 24.8 cm in diameter. The bulk density and tensile strength of the target were 1.08 g/cm^3 and 2.4 MPa, respectively. A nylon sphere with 3.2 mm in diameter impacted into the target at ~3.4 km/s. The ratio of the radius of projectile and target (the normalized curvature) are 0.013-0.041. The targets were placed in a styrofoam box, and the target and their fragments were collected from the box in each shot. The spherical surface including a resultant crater was scanned by a high resolution 3-D geometry measurements system (COMS MAP-3D). The volume and depth of the crater was measured with the deviation from the pre-impact surface determined by the topographic data around the crater. The radius of a circle having an area equal to the area occupied by craters on the pre-impact surface was defined as the crater radius.
The resultant craters consist of a circular pit and a spall region around the pit. A larger target curvature led to a broader the spall region. The volume and diameter of the crater increase with the target curvature, although the depth of the crater is almost constant. The volume of spall region and the crater profiles also show that the spall region gets broader and deeper with the target curvature. The volume increase in the spall region mainly contributes to the volume increase of the crater.
We developed a model focusing on the normal component of the force to the target surface without taking into account of the interference zone. The experimental results fell in the area constrained by model curves with reasonable parameters (the radius of the isobaric core and the attenuation rate of the impact induced pressure) on the diagram of the ratio of the crater radius to those on plane surface and

the target curvature. Namely, the distance from the equivalent center to the target free surface is shorter for higher curvature, which mainly contributes to the increase of the crater diameter and volume with the target curvature. The curvatures for some largest craters on the asteroids are within the range of the curvature in this study. The increase of the crater radius originated from the curvature might have to be considered for spall craters in their size range.

Keywords: impact craters, impact experiments, small bodies, morphology, two-stage light-gas gun

JUICE/GALA-J (2): Science targets of the GAnymede Laser Altimeter (GALA) for the JUICE mission

*Jun Kimura[1], Shunichi Kamata[2], Koji Matsumoto[3], Shoko Oshigami[8], Noriyuki Namiki[3], Kiyoshi Kuramoto[2], Sho Sasaki[1], Keigo Enya[4], Masanori Kobayashi[5], Shingo Kobayashi[6], Hiroshi Araki[3], Hirotomo Noda[3], Ko Ishibashi[5], Yoshifumi Saito[4], Hauke Hussmann[7], Kay Lingenauber[7]

1. Osaka University, 2. Hokkaido University, 3. National Astronomical Observatory Japan, 4. Institute of Space and Astronautical Science, 5. Chiba Insitute of Technology, 6. National Institute of Radiological Sciences, 7. Deutsches Zentrum für Luft- und Raumfahrt, 8. Kogakuin University

The JUpiter Icy Moons Explorer (JUICE), led by European Space Agency, has started development toward launch in 2022 (arrival at Jupiter in 2029, and Ganymede orbit insertion in 2032), and we are now developing the GALA instrument onboard JUICE spacecraft collaborating with German Aerospace Center (DLR) and other institutions in Europe. GALA will acquire the key information for understanding the evolution of Jovian icy moons and to play an essential role in the JUICE's purpose: exploration of deep habitat.

Jovian icy moon Ganymede, which is the largest moon in the Solar System and the primary target of the JUICE, can be said to be one of the typical solid bodies along with terrestrial planets in terms of its size and the intrinsic magnetic field originated from the metallic core. However, current knowledge provided by previous explorations is extremely limited since it comes from only several fly-bys. The JUICE will unveil the whole picture of Ganymede by the first orbiting in the history around extra-terrestrial moon. Expected new big picture of the origin and evolution of Ganymede will not only be a key to unveil the origin of diversity among the Solar System bodies, but also contribute to an understanding of exoplanets with a wide diversity.

The GALA will measure a distance between the spacecraft and the surface of icy moons and acquire the topography data (globally for Ganymede, and fly-by region for Europa and Callisto). It will be a first-ever laser altimetry for the icy object. Such information makes surface geologies clear and tremendously improves our understanding of the icy tectonics. By comparing their tectonic styles on the rocky planets/moons, GALA data leads to reconsider the Earth's plate tectonics. In addition, the GALA will confirm a presence/absence of the subsurface ocean by measuring tidal and rotational response, and the gravitational information reflecting the interior structure will be greatly improved. Furthermore, strength and waveform of reflected laser pulse have an information about surface reflectance at the laser wavelength and small-scale roughness. Finally we can see degrees of erosion and space weathering without being affected by illumination condition through GALA measurements.

In order to interpret and understand such measurements, accumulated studies for the Earth over the years will be effectively utilized: e.g., the data for surface topography, roughness and albedo will lead to describe the icy tectonics through the knowledge from terrestrial glaciology and experiments on impact and deformation process. The tidal measurements by GALA will also be a window to see its interior based on our knowledge and experiences cultivated through the past geodetic observations, e.g., the SELENE mission for the terrestrial Moon.

Characterization of the icy moons will be achieved not only from the GALA measurements but also synergy of other scientific instruments onboard JUICE spacecraft, for examples, surface images taken by optical camera (JANUS) will confirm the position of GALA laser footprint to complement the GALA "point" data for precise topographic mapping. A radar sounder (RIME) and a radio science experiment (3GM) probe the interior structure, especially interior of the icy crust to figure out an occurrence of tectonic features. A visible and infrared imaging spectrometer (MAJIS), an ultraviolet imaging spectrograph (UVS) and a

sub-millimeter wave instrument (SWI) will acquire a surface and atmosphere compositional data. A magnetometer (J-MAG) monitors moons' inductive response to the Jovian magnetic field and probes the subsurface ocean with the help of a particle environment package (PEP) and a radio and plasma wave investigation (RPWI). The GALA works closely together with these instruments and plays a leading and a supporting role to clarify the whole picture of Ganymede and other icy moons.

Period characteristics of Mercury's external magnetic field from MESSENGER magnetometer observation

*Takaaki Katsura[1], Hiroaki TOH[2]

1. Solar-Planetary Electromagnetism Laboratory, Department of Geophysics, Graduate School of Science, Kyoto University, 2. Data Analysis Center for Geomagnetism and Space Magnetism Graduate School of Science, Kyoto University

MESSENGER(MErcury Surface, Space Environment, Geochemistry, and Randing) is the first probe launched into Mercury centric orbit and has been observed electromagnetic circumstances including magnetic field over about four years since 2011.From this data the average shape and location of Mercury’s magnetopause and bow shock have determined (Winslow et al., 2013).Furthermore, from the studies of magnetic fields induced at the top of Mercury’s core by time-varying magnetospheric fields, the radius of Mercury’s core is determined (Johnson et al., 2016).

At present, however for the period of external magnetic variations, annual variation due to Mercury’s high orbital eccentricity alone is considered. In general more precision information about conductivity structure of planetary bodies e.g. separation of the thickness and conductivity of spherical body (or shell) would be expected to be given by multi-frequency sounding. Accordingly we forcus on subsolar distance as an index of the time variation of Mercury's external magnetic field in order to estimate the period characteristics of external field. Since magnetopause is determined by the balance between planetary intrinsic magnetic field and solar wind, subsolar distance is able to be regarded as an index of the variation of external magnetic field.

We identify the location of Mercury's magnetopause from vector magnetic field data by MESSENGER observation in fifteen Mercury years and study the period characteristics of Mercury's external magnetic field by converting the data of magnetopause into that of subsolar distance and analyzing the time-variation of them, and report the result.

Keywords: Mercury, MESSENGER, Magnetopause

Measurement of crater ray length by analysis of lunar images: A comparison with Z model

*Kinoshita Toshiki[1], Akiko Nakamura[1], Koji Wada[2]

1. Department of Planetology, Graduate School of Science , Kobe University, 2. Planetary Exploration Research Center, Chiba Institute of technology

The information of impactor, such as impact velocity, density, or radius, is coupled into a coupling parameter C (Holsapple and Schmidt, 1987) and cannot be resolved from crater diameter only. In order to examine if we can put constraints on the information of impactor by spatial extent of ejecta, i.e., the distribution of continuous ejecta and length of ray, we performed quantitative measurement of ejecta. We analyzed images provided by Multiband Imager (MI) onboard the JAXA’s lunar orbiter, Kaguya. We analyzed 13 small craters in the southwestern region of Kepler crater on Oceanus Procellarum. First, we tried to define the region to which we could apply Z model. We measured the circularity of the area with a reflectance higher than a set-value. In the figure, the horizontal axis shows the equivalent diameter of a circle of the region and the vertical axis shows the circularity. As the reflectance increases, the circularity of the region increases. The slope changes at the diameter roughly 4 times as large as the crater diameter. From this result, we regarded that the Z model is applicable to the region within about 4 crater radii from the crater center. In the region beyond about 4 crater radii, ejecta inelastically collided one another, became collimated in discrete directions, and deposited in rays (Kadono et al., 2015). In other words we assumed that the rays next to each other had shared the ejecta released in the direction in between. Based on this assumption, we calculate the thickness of ejecta in each ray using the angles between rays on the MI images, the width of rays, and Z model, and will discuss on its relationship with the crater diameter.

Keywords: crater ray, ejecta, Kaguya

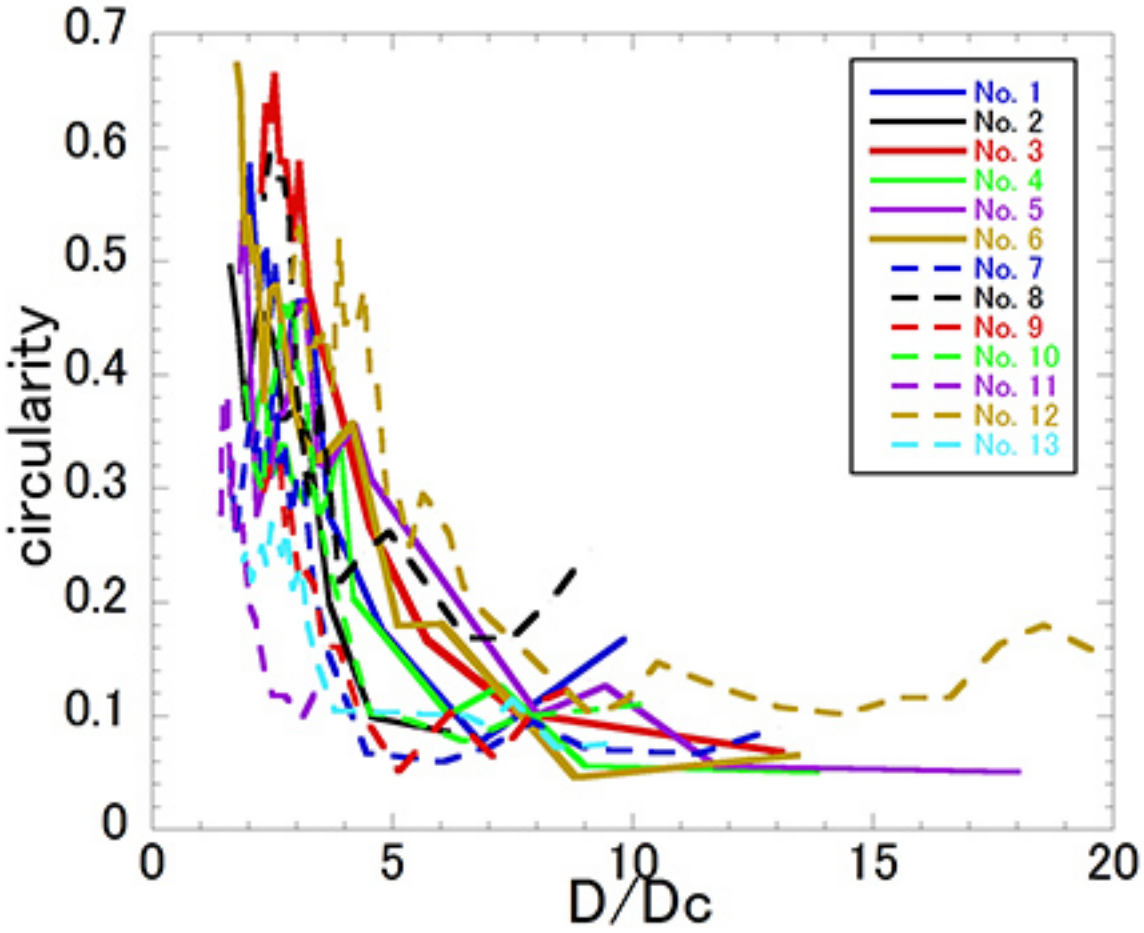

Correct correspondence selection between points on two asteroid images using epipolar constraint

*Junpei Ohyama[1], Naoya Ohta[1], Naoko Ogawa[2]

1. Gunma University, 2. Japan Aerospace Exploration Agency (JAXA)

In asteroid exploring missions like HAYABUSA 2, it is often needed to compute the shape of the target asteroid using its images taken after the space craft arrives at the asteroid. In this computation process, correspondences between points on two images taken from different view direction have to be established. In order to accomplish this task automatically, we first extract image features from the two images using image processing techniques, and compute matched pairs of them based upon similarity of the features. However, this similarity based matching produces relatively high rate of wrong correspondence. However, if we use epipolar constraint, which gives the relation between image positions of an object point on two images taken from different view points, it is expected that we can reduce the error rate of the correspondence. This report states the experimental results of this approach. In the experiments, we used images of an asteroid model made in JAXA, and AKAZE (Alcantarilla et al. 2013) as the image feature. The correct matches were selected by human eyes as the ground truth. In the case that the correct matching rate is 68 percents when using only the feature similarity, the correct matching rate increased to 97 percents when using epipolar constraint too. This result suggests using epipolar constraint is effective when establishing feature correspondence between two asteroid images.

Keywords: epipolar constraint, fundamental matrix, asteroid image, point correspondence, AKAZE

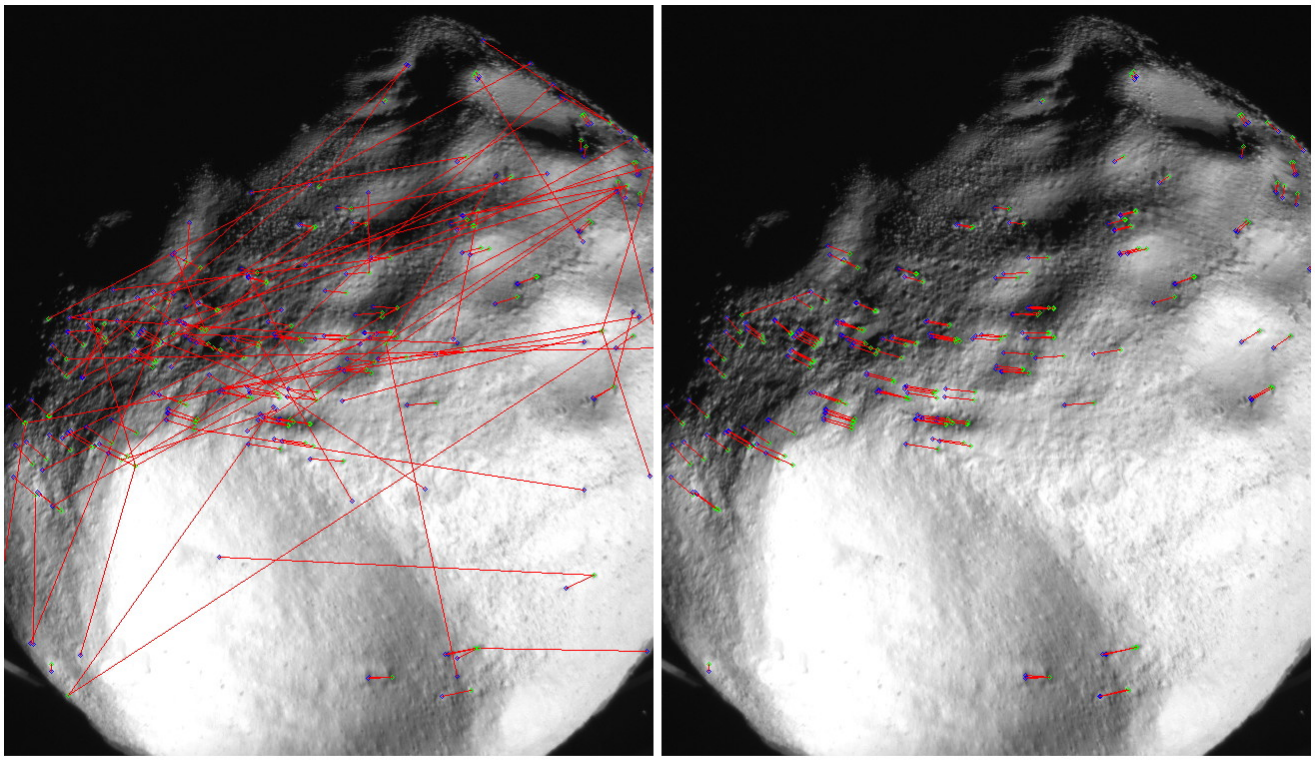

correspondances without epipolar constraint correspondances with epipolar constraint

Performance comparison between SIFT and AKAZE for corresponding point computation on asteroid images

*Hiroki Yamaguchi[1], Naoya Ohta[1], Naoko Ogawa[2]

1. Gunma University, 2. Japan Aerospace Exploration Agency (JAXA)

In asteroid exploring missions like HAYABUSA 2, it is often needed to compute the shape of the target asteroid using its images taken after the space craft arrives at the asteroid. In this computation process, correspondences between points on two images taken from different view direction have to be established. In order to accomplish this task automatically, image features computed by image processing techniques are used. Among many image features, it is reported that SIFT (Lowe 2004) has good performance for the current purpose (Takeishi et al. 2015). However, SIFT is protected by patent and this can be an obstacle for some situations. On the other hand, AKAZE (Alcantarilla et al. 2013), which was proposed after SIFT, has no limitation in its usage. So, we have compared the performances of SIFT and AKAZE when using them to asteroid images. In the experiments, images of an asteroid model made in JAXA were used. The number of feature points detected by SIFT (e.g. around 6000) is greater than that by AKAZE (e.g. around 3000), but even the number of points by AKAZE is enough amount for the current purpose. The error rates by SIFT and AKAZE for the correspondence computation between two images taken from different view angles are almost the same (e.g. 30 to 40 percents), and sometime the error rate by AKAZE becomes smaller the rate by SIFT (e.g. 32 vs. 36 persents). From these experimental results, we conclude AKAZE has enough performance for correspondence computation for asteroid images.

Keywords: SIFT, AKAZE, asteroid image, feature point, point correspondence

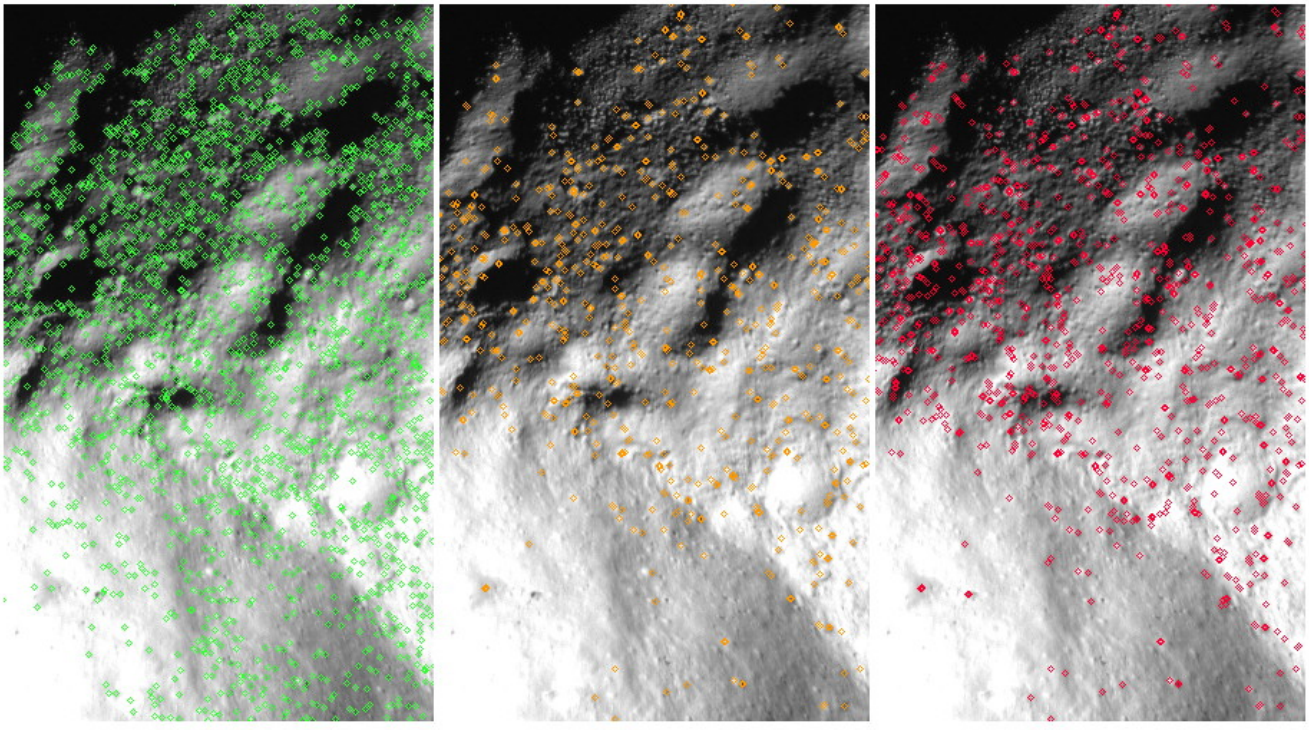

feature points by SIFT | common feature points | feature points by AKAZE

Near-Infrared Photometry of Near Earth Asteroid (1566) Icarus and 2007 MK6

*Yuri Sakurai[1], Seitaro Urakawa[2], Jun TAKAHASHI[3], Tomoyasu TANIGAWA[4], Sayuri NAKAMURA[5], George HASHIMOTO[1]

1. Department of Earth Sciences, Okayama University, 2. Japan Spaceguard Association, 3. University of Hyogo, 4. Sanda Shounkan Highschool, 5. Okayama University

Rotation period of Near Earth Asteroid (1566) Icarus is estimated to be 2.2726 hours (Warner, 2015). Since Icarus' rotation rate is just below the threshold for breakup via centrifugal force, breakup of Icarus might have occurred in the near past. Ohtsuka et al. (2007) found a dynamical relationship between Icarus and 2007 MK6, and proposed that 2007 MK6 is likely a family member of Icarus. To examine the Icarus' breakup hypothesis, we observed Icarus and 2007 MK6 at Nishi-Harima Astronomical Observatory with the Nishiharima Infrared Camera (NIC) which is a near infrared simultaneous three-band (J, H, and Ks) camera.
The observation of Icarus was done between 2015 June 18 and 21, and the observation of 2007 MK6 was done between 2016 June 15 and 18. For a flux calibration, we also observed nearby stars of spectral type G2V, and their magnitude were derived from the 2MASS database. The Icarus' breakup hypothesis was tested by a comparison of near infrared colors of Icarus and 2007 MK6.

Keywords: Asteroid, Photometry, Near-Earth Objects

Observation of near-earth object (1566) Icarus and the split candidate 2007 MK6

*Seitaro Urakawa[1], Katsutoshi Ohtsuka[2], Shinsuke Abe[3], Daisuke Kinoshita[4], Hidekazu Hanayama[5], Takeshi Miyaji[5], Shin-ichiro Okumura[1], Kazuya Ayani[6], Syouta Maeno[6], Daisuke Kuroda[5], Akihiko Fukui[5], Norio Narita[5,7,8], George HASHIMOTO[9], Yuri SAKURAI[9], Sayuri Nakamura[9], Jun Takahashi[10], Tomoyasu Tanigawa[11], Otabek Burhonov[12], Kamoliddin Ergashev[12], Takashi Ito[5], Fumi Yoshida[5], Makoto Watanabe[13], Masataka Imai[14], Kiyoshi Kuramoto[14], Tomohiko Sekiguchi[15], MASATERU ISHIGURO[16]

1. Japan Spaceguard Association, 2. Tokyo Meteor Network, 3. Nihon University, 4. National Central University, 5. National Astronomical Observatory of Japan, 6. Bisei Observatory, 7. Astrobiology Center, 8. University of Tokyo, 9. Okayama University, 10. University of Hyogo, 11. Sanda Shounkan Highschool, 12. Ulugh Beg Astronomical Institute Uzbekistan Academy of Science , 13. Okayama University of Science, 14. Hokkaido University, 15. Hokkaido University of Education, 16. Seoul National University

Background & Aim: A numerical simulation proposes that the origin of near-Earth object 2007 MK_6 (hereafter, MK6) is a near-Earth object (1566) Icarus (hereafter, Icarus) [1]. In addition to it, the orbital parameters of the daytime Taurid-Perseid meteor swarm are in good agreement with those of Icarus. Thus, it is considered that MK6 is split from the parent object Icarus by a rotational fission and/or an impact event, and the produced dust became to the daytime Taurid-Perseid meteor swarm. To confirm such a hypothesis, we need to obtain the observational evidence that the color indices of Icarus and MK6 are same. Moreover, if MK6 split by the rotational fission due to the YORP effect, the rotation period of Icarus would be shorten compared with the past rotation period. When the MK6 split by an impact event, the rotation period of MK6 would shorter than the spin limit of 2.2 hours. We require the observation for Icarus and MK6 to test these hypotheses.

Observations: We conducted the observations for Icarus in 2015 and MK6 in 2016, respectively. The observation summary is shown as followings: Icarus (June 2015): Nayoro Observatory 1.6 m Pirka telescope of the Hokkaido University (visible photometry), Ishigakijima Astronomical Observatory (IAO) 1.05 m Murikabushi telescope (g', R_C, and I_C band simultaneous photometry), Maidanak Observatory (MO) 0.6 m telescope (R band photometry), Nishi-Harima Astronomical Observatory (NHAO) Nayuta 2.0m telescope (J, H, and K_S band simultaneous photometry), Lulin and Kinmen Observatory 0.4 m telescopes (visible photmetry), Lowell Observatory (LO) 1.1 m, 1.8 m, and 4.3 m telescopes (visible photometry and visible spectroscopy), MK6 (June - July 2016): IAO 1.05 m Murikabushi telescope (g', R_C, and I_C band simultaneous photometry), MO 1.5 m telescope (R band photometry), NHAO Nayuta 2.0 m telescope (J, H, and K_S band simultaneous photometry), Lulin Observatory 1.0 m telescope (visible photometry), LO 1.8 m and 4.3 m telescopes (visible photometry and visible spectroscopy), University of Hawaii 2.24 m telescope (visible photometry), Okayama Astrophyscial Observatory 1.88 m telescope (g', r', and z' band simultaneous photometry).

Results: Previous studies indicated that the taxonomic type of Icarus is an S-type or a Q-type [2][3]. We obtained that the color indices $g' - R_C$ and $R_C - I_C$ are 0.828 ±0.027 mag and 0.397 ±0.025 mag, respectively. These are consistent with the color indices of an S-type asteroid. Moreover, the color indices implied the slight rotational color variation, though the further data analysis is needed. On the other hand, the color indices and the rotation period of MK6 have not been revealed in the previous study. In addition to the color indices of Icarus, we will present the result the color indices of MK6 and the rotation period of both Icarus and MK6.

References: [1] Ohtsuka K. et al. (2007) *ApJ*, *668*, L71-L74. [2]Chapman C. R., Morrison D., and Zellner B. (1975) *Icarus*, *25*, 104-139. [3]Hicks M. D., Fink U., and Grundy W. M. (1998) *Icarus, 133,* 69-78.

Keywords: Asteroids, Photometry, Near-Earth Objects

Sintering of icy dust aggregates due to turbulence in a protoplanetary disk

*Kiriko Kodama[1], Sin-iti Sirono[1]

1. Graduate School of Environmental Studies, Nagoya University

In a protoplanetary disk, coagulation of dust grains is the first step of planetary formation. It is important to know whether dust grains can grow or not. There are two types of dust grains. One is made of ice and the other of rock. In this study, we focus on icy dust grains. Icy dust aggregates are sintered when they are heated. Sintering is the material transfer phenomenon to decrease total surface area. When an icy dust aggregate is sintered, necks connecting dust grains grow. Because collision between sintered aggregates results in bouncing, they cannot grow. Hence, sintering greatly affects the first step of planetary formation.
The heat source is visible light irradiation from the central star in a protoplanetary disk. Because the dust grains around at the midplane blocks the irradiation, only dust grains around the surface of a disk can be heated. Therefore, if turbulence transports an icy dust aggregate to the surface having high temperature, sintering can proceed.
Using radial temperature distribution at the midplane, a timescale required for sintering was estimated by Sirono (2011, ApJ, 735, 131). However, this study did not take account of the vertical motion of icy dust aggregates. In this study, we calculate the vertical motion of each aggregate to clarify the sintering timescale shortened by turbulent diffusion.
The vertical motions of dust aggregates are diffusion by turbulence and sedimentation by gravity of the central star. Distribution of dust aggregates reaches a steady state in the sedimentation timescale. In the steady state condition, each aggregate moves up and down in a vertical direction of a protoplanetary disk, icy dust aggregates are sintered if they exceed the altitude of high temperature. We calculated the position of aggregates as a function of time. Because sintering strongly depends on temperature (Sirono, 2011, ApJ, 735, 131), sintering of icy dust aggregates can be assumed to quickly proceed at a particular height from the midplane. By numerical simulation we calculated the fraction of sintered dust aggregates that experienced high temperature. The fraction of sintered dust aggregates increases with time. From this fraction, the sintering timescale is determined.
It is found that the sintering timescale gets shorter as the altitude of high temperature decreases. If it falls to the dust aggregate disk scale height, the sintering by turbulent diffusion proceeds enough. The altitude of high temperature depends on opacity of aggregates. If the opacity goes down as dust aggregates grow, the new sintering region appears. However, if a little small dust aggregates are present, the height can hardly fall down. Therefore, the sintering by transporting to disk surface does not proceed.

Keywords: protoplanetary disk, sintering, turbulence

Distribution of captured planetesimals in circumplanetary disks and implications for accretion of regular satellites

*Ryo Suetsugu[1], Keiji Ohtsuki[2]

1. University of Occupational and Environmental Health, 2. Kobe University

Regular satellites of giant planets are formed by accretion of solid bodies in circumplanetary disks. Planetesimals that are moving on heliocentric orbits and are sufficiently large to be decoupled from the flow of the protoplanetary gas disk can be captured by gas drag from the circumplanetary disk. In the present work, we examine the distribution of captured planetesimals in circumplanetary disks using orbital integrations. We find that the number of captured planetesimals reaches an equilibrium state as a balance between continuous capture and orbital decay into the planet. The number of planetesimals captured into retrograde orbits is much smaller than those on prograde orbits, because the former ones experience strong headwind and spiral into the planet rapidly. We find that the surface number density of planetesimals at the current radial location of regular satellites can be significantly enhanced by gas drag capture, depending on the velocity dispersions of planetesimals and the width of the gap in the protoplanetary disk. Using a simple model, we also examine the ratio of the surface densities of dust and captured planetesimals in the circumplanetary disk, and find that solid material at the current location of regular satellites can be dominated by captured planetesimals when the velocity dispersion of planetesimals is rather small and a wide gap is not formed in the protoplanetary disk. In this case, captured planetesimals in such a region can grow by mutual collision before spiraling into the planet, and would contribute to the growth of regular satellites.

Keywords: planets and satellites

Temporary Capture of Small Bodies by an Eccentric Planet

*Arika Higuchi[1], Shigeru Ida[2]

1. Tokyo Institute of Technology, 2. Earth-Life Science Institute

We have investigated the probability of temporary capture of asteroids in eccentric orbits by a planet in a circular or an eccentric orbit by analytical and numerical calculations. We found that in the limit of the circular orbit, the capture probability is ~0.1% of encounters to the planet's Hill sphere, independent of planetary mass and semimajor axis. In general, the temporary capture becomes difficult, as the planet's eccentricity (e_p) increases. We found that the capture probability is almost independent of e_p until a critical value (e_p^c) that is given by ~5 times of Hill radius scaled by the planet's semimajor axis. For $e_p > e_p^c$, the probability decreases approximately in proportional to e_p^{-1}. The current orbital eccentricity of Mars is several times larger than e_p^c. However, since the range of secular change in Martian eccentricity overlaps e_p, the capture of minor bodies by the past Mars is not ruled out.

Keywords: Martian moons, asteroids

Position of Snow Line Depending on Spatial Distribution of Magnetorotational Instability in Protoplanetary Disks

*Shoji Mori[1], Satoshi Okuzumi[1]

1. Department of Earth and Planetary Sciences, Tokyo Institute of Technology

Icy dust plays important role of planetesimal formation in protoplanetary disks because it dominates mass of the solid material. In addition, because icy dust is also related to origin of ocean of rocky planets, to understand spatial distribution of icy dust is essential for not only planet formation but also origin of life. Icy dust is present beyond sublimation boundary of H^2O ice (snow line). Therefore, to understand radial temperature profile which determines position of snow line is particularly important. Before the disk dissipating, at the inner region in which snow line lies is optically thick, gravitational energy of accreting gas is converted by turbulent viscosity to heat accumulated onto the disk. The heat determines the temperature profile. That is this viscous heating controls the position of snow line (Oka et al. 2011).

The turbulence in protoplanetary disks is driven by an instability (magnetorotational instability) caused by interplay between disk magnetic fields and ionized gas. Growth of magnetorotational instability causes vigorous turbulence, although it needs sufficient ionization fraction of the disk. Therefore, at high density region of too low ionization fraction, magnetorotational instability is stable. In that region, magnetic turbulence would not be generated.

When one considers the viscous heating, heating rate distribution concentrating on midplane is often assumed. However, in the stable region, because absence of turbulence, the turbulent viscosity generates heat at the upper layer (Hirose & Turner 2011). Since viscous heating increases the midplane temperature by accumulation of heat into optically thick region, heat at the upper layer leads to lower midplane temperature than heating at midplane.

In this work, focusing on this fact, we investigate temperature profile based on distribution of magnetic turbulence and the position of snow line. Specifically, we perform three dimensional magnetohydrodynamics simulation including stratification and ionization fraction distribution. As a result, we confirm that peak of the heating rate is located at 3 scale height from midplane. This is consistent with Hirose & Turner (2011). We calculate the position of snow line assuming the accreting heating releases at 3 scale height. As a result, in the case of accretion rate of 10^{-8} M_{solar}/year, snow line of 3 AU with midplane heating changes to snow line of 0.7 AU with upper layer heating. Thus, the distribution of magnetic turbulence would control position of snow line. We also investigate dependence of initial magnetic field strength on the dissipation rate distribution and discuss the position of snow line depending on the initial magnetic field strength.

Keywords: Protoplanetary disk, Magnetohydrodynamics, Snow line

Numerical simulation of Saturn ring formation using SPH

*keiya murashima[2], Natsuki Hosono[1], Yosuke Yamashiki[1]

1. Global Water Resources Assessment Laboratory - Yamashiki Laboratory Graduate School of Advanced Integrated Studies in Human Survivability Kyoto University, 2. Faculty of Science, Kyoto University

The origin of Ring formation of Saturn is well explained by Ripped-apart icy moon hypothesis proposed by Canup et al.,in which Saturn's planetary tidal forces preferentially strip material from the Titan-sized icy moon’ s outer icy layers, while its rocky core remains intact and is lost to collision with the planet.
We performed numerical simulations using SPH and surveyed the effect of the initial conditions and dependance of the number of particles to the results. We will show the the result of numerical simulations which includes the material strength.

Keywords: Ripped-apart icy moon, SPH, propeller structure

Ring formation around giant planets by tidal disruption of a passing large Kuiper belt object

*Ryuki Hyodo[1,2,3], Sebastien Charnoz[2], Keiji Ohtsuki[3], Hidenori Genda[1]

1. Earth-Life Sicence Institute, Tokyo Institute of Technology, 2. Institut de Physique du Globe de Paris, 3. Graduate School of Science, Kobe University

The origin of rings around giant planets remains elusive. Saturn's rings are massive and made of 90–95% of water ice with a mass of ~10^{19} kg. In contrast, the much less massive rings of Uranus and Neptune are dark and likely to have higher rock fraction. According to the so-called “Nice model”, at the time of the Late Heavy Bombardment, giant planets could have experienced a significant number of close encounters with bodies scattered from the primordial Kuiper Belt. This belt could have been massive in the past and may have contained a larger number of big objects ($M_{body}=10^{22}$ kg) than what is currently observed in the Kuiper Belt. Here we investigate, for the first time, the tidal disruption of a passing object, including the subsequent formation of planetary rings. First, we perform SPH simulations of the tidal destruction of big differentiated objects ($M_{body}=10^{21}$ and 10^{23} kg) that experience close encounters with Saturn or Uranus. We find that about 0.1–10% of the mass of the passing body is gravitationally captured around the planet. However, these fragments are initially big chunks and have highly eccentric orbits around the planet. In order to see their long-term evolution, we perform N-body simulations including the planet's oblateness up to J_4 starting with data obtained from the SPH simulations. Our N-body simulations show that the chunks are tidally destroyed during their next several orbits and become collections of smaller particles. Their individual orbits then start to precess incoherently around the planet's equator, which enhances their encounter velocities on longer-term evolution, resulting in more destructive impacts. These collisions would damp their eccentricities resulting in a progressive collapse of the debris cloud into a thin equatorial and low-eccentricity ring. These high energy impacts are expected to be catastrophic enough to produce small particles. Our numerical results also show that the mass of formed rings is large enough to explain current rings including inner regular satellites around Saturn and Uranus. In the case of Uranus, a body can go deeper inside the planet's Roche limit resulting in a more efficient capture of rocky material compared to Saturn's case in which mostly ice is captured. Thus, our results can naturally explain the compositional difference between the rings of Saturn, Uranus and Neptune.

This work is published in Hyodo,R.,Charnoz,S.,Ohtsuki,K.,Genda,H. 2017, Icarus, 282, 195-213.

Keywords: Rings, Satellites, Giant planets

Effect of Planetary Spin on Giant Impacts

*Natsuki Hosono[1,2], Eiichiro Kokubo[3]

1. Kyoto University, 2. RIKEN, 3. NAOJ

In planetary science, impact phenomena between two objects play an important role, e.g., the Moon-forming impact.
Thus, to date, a lot of numerical simulations of giant impacts are carried out.
A potentially important effect on giant impacts is the spin of colliding bodies.
However, most previous works neglected the spin.
It is more natural that the bodies have pre-impact rotations.
In this work, we systematically investigate the effect of the spin on giant impacts.
We employ the Density Independent SPH, which is an improved version of the standard SPH method.
We show the dependence of the collisional outcome on the spin period.

The Origin of Asteroid Geometries: Dependence on Conditions of Planetesimal Collisions

*Keisuke Sugiura[1], Shu-ichiro Inutsuka[1], Hiroshi Kobayashi[1]

1. NAGOYA UNIVERSITY Graduate School of Science

Recent observations by space probes or light curves clarify that most of asteroids in present solar system have irregular shapes distinctly different from a sphere, such as asteroid Itokawa. These irregular shapes are supposed to be created by collisional destruction and coalescence of planetesimals. We expect that we can clarify the past environment of the solar system if we clarify the relationship between impact condition, such as impact angle or velocity, and resultant irregular shape of planetesimal, and compare with the asteroid shapes in present solar system.
For relatively small objects like planetesimals, effect of material strength or friction is also important other than effect of the self-gravity. To investigate the resultant shape of planetesimals made by collisional destruction and re-accumulation, we developed numerical simulation code of Smoothed Particle Elastic Dynamics (Sugiura and Inutsuka 2016, 2017). Moreover, we included fracture model (Benz and Asphaug 1995) and friction model (Jutzi 2015) to describe realistic property of rocks. Owing to friction model, we can represent the irregular shape of rubble pile formed by re-accumulation of fragments. Our simulation code also calculates the self-gravity, and thus we can treat collisional destruction and subsequent gravitational re-accumulation consistently.We simulate the collision between rocky planetesimals with the radius of about 50 km while varying the impact velocity, impact angle and mass ratio, and we measure the axis ratios of fragments with sufficiently high resolution. In this talk, we will discuss the relationship between resultant shape of planetesimals and impact condition, and mechanism to produce irregular shapes.

Keywords: asteroid geometry, planetesimal collision, SPH, elastic dynamics

Impact cratering on a silica dust layer with high porosity and the effect of porosity on the crater size scaling law

*Takuya Ishiguro[1], Masahiko Arakawa[1]

1. Graduate School of Science, Kobe University

Recent planetary exploration revealed that small bodies in the solar system could have a large porosity as large as 80% for comet nuclei and less than 75% for asteroids. Impact craters found on such highly porous bodies were recognized to be quite different from that found on rocky bodies without porosity, that is, there were several craters on their surface which sizes were beyond their radius. These large craters were supposed to be formed by pore collapse during the impact compression and so it was recently classified into a compressive type crater. Classically, the impact crater is classified into two types depending on the physical mechanism controlling the final crater size: they are a crater formed in a gravity dominated regime and a crater formed in a strength dominated regime. These classical type crates have been studied to construct the crater size scaling law, and now the p scaling law was widely accepted to use for the planetary impact phenomena. However, the effect of porosity on this p scaling law for the crater size was not clarified yet although limited studies have been conducted by Housen and Holsapple (2003) and others. The π scaling law applicable for the porous asteroids is necessary for the impact experiment on small asteroid Ryugu by Hayabusa-2 small carry-on impactor because one candidate for the surface condition on Ryugu is fine-grained layer with a high porosity.
In this study, commercial amorphous silica dusts with the average particle size of 0.5mm and the density of 2.2gcm^{-3} (ρ) were used to prepare the target with the bulk porosity from 50% to 78%, and the target was simply consolidated by the cohesion force of Van Der Waals force with the tensile strength from 100 Pa to 10^4 Pa. We made impact cratering experiments using this porous target to study the effect of the porosity on the crater morphology including the crater size. Impact experiments were conducted by using a horizontal type two-stage light gas gun set at Kobe University and a glass bead projectile with the diameter of 2mm and the mass of 10 mg (m_p) was launched at the impact velocity at 3.60 kms^{-1}. The projectile was impacted on the target surface normally set in a large vacuum chamber less than 20 Pa. The crater morphology was found to change with the increase of the porosity, that is, the shallow dish type crater was observed on the target with the porosity of 50% having the tensile strength of 10^4 Pa, and as the porosity increased the impact spherical cavity was formed to grow and expanded below the shallow dish crater. The recovered target was hardened by epoxy resin and cut at the center of the crater to observe the cross section to measure the cavity diameter (D), the depth of the crater (d) and the diameter of the shallow dish crater. The relationship between the distension ($a=\rho / \rho_{bulk}$) and the normalized cavity diameter, $\pi_D=(\rho_{bulk} D/m_p)^{1/3}$, was found to follow the empirical equation of $\pi_D=3.8a^{0.7}$, where r_{bulk} is bulk density of the target, and the relationship between the distension and the normalized depth, $\pi_D=(\rho_{bulk} d/m_p)^{1/3}$, was found to follow the empirical equation of $\pi_D=3.0a^{1.0}$. While the crater diameter of the shallow dish crater found at the entrance of the cavity was recognized to be constant irrespective of the porosity. These empirical equations could be used to incorporate the effect of porosity on the crater size scaling law.

Keywords: Impact crater, scaling law, porous bodies

Probability distribution of impact strength on the target simulating meteorites and implication for the size dependence of asteroid strength

*Fumiya Nagatomo[1], Masahiko Arakawa[1], Chisato Okamoto[1]

1. Graduate School of Science, Kobe University

Impact strength of asteroids is one of the most important physical parameter to control the size frequency distribution of asteroids in the main belt. The impact strength has been studied in the laboratory using cm-scale targets simulating various type asteroids such as rocky, icy and metal bodies, and these previous studies revealed that the impact strength strongly depended on materials and internal structure such as porosity. However, actual collision among asteroids happen at the scale of several orders of magnitude larger than that at the laboratory scale. Therefore, the size dependence of the impact strength is quite important to consider the asteroid collision. There is a traditional theory for material strength and it is well known that the material strength follows probability distribution: it scatters according to Weibull distribution. This probability distribution of the material strength is theoretically connected to the size dependence of the material strength: so called the Weibull statistical fracture theory. This size dependence is confirmed at the static deformation condition so far, then we try to extend this Weibull theory to the dynamic deformation condition corresponding to high-velocity impact for the purpose of asteroid collisions.

We made impact disruption experiments by using a vertical type gas gun set at Kobe University. A nylon ball projectile with the diameter of 10mm was launched at the velocity from 65 to 208 ms^{-1}, and was impacted on the target surface normally. The targets were a gypsum-glass beads mixture (GG) with the mean density of 1.9gcm^{-3} or a gypsum-bentonite mixture (GB) with the mean density of 0.77 gcm^{-3}; both had a shape of cylinder whose dimeter was 30mm. CG and GB targets were analogues of chondritic meteorites, so the glass beads with the size of 1mm simulated a chondrule. The impact experiments were conducted 10 times at the same impact condition for each target: the constant energy density (Q: the kinetic energy of projectile divide by target mass) was applied to the target, and we measure the mass of the largest fragment (LFM) at each time, then we noticed that the resultant 10 data were so scattered. We studied the probability distribution of the largest fragment mass, and then we obtained the impact strength (Q^*) from the largest fragment mass on the basis of the typical relationship between LFM and Q. Impact experiments at two different energy densities were conducted for each target. We also measured the tensile strength of GG and GB targets more than 10 times by the static deformation test to study the probability distribution of the tensile strength.

We obtained the Weibull parameter (Φ) to characterize the probability distribution of the strength for the tensile fracture: Φ=7 and 8 for GG and GB target, respectively; they are similar to the values obtained for basalt and granite. The cumulative probability, P, of the fracture for the materials is shown as follows according to the Weibull theory, $P=1-\exp(-V/V_0(\sigma/\sigma_0)^{\Phi})$ (eq.1), where V is volume of the target and σ is strength, and the suffix 0 shows the standard condition. The largest fragment mass recovered from impact experiments was found to scatter so much; e.g. GG target showed the scattering in one order of magnitude. The average impact strength of GG and GB target for 20 experiments in each was obtained to be 34 and 158 Jkg^{-1}, respectively, and we tried to make the relationship between P and Q^* according to eq.1 by substituting Q^* for σ, where Q^* was determined from each LMF using the typical relationship between LFM and Q, then $\Phi$was obtained from the probability distribution of the impact strength: $\Phi$is 1.8 and 2.6 for GG and GB target. Thus, the size dependence of the impact strength could be estimated from

eq.1 setting P=0.5: $Q^*=Q_0 D^{-n}$, where D is the target size and n is 1.6 and 1.2 for GB and GG target, respectively.

Keywords: Impact strength, Impact scaling law, Asteroids

High-velocity impact cratering experiments on granular layer with various water contents

*Taku Tazawa[1], Masahiko Arakawa[1], Kazuma Matsue[1]

1. Graduate School of Science, Kobe University

Recent study on numerical simulations of large scale impact cratering showed that complex crater such as a central-peak type crater was formed within the region where the materials composing the surface crust lost their shear strength by high shock pressure, and that this fluidized region should have a rheological property like Bingham fluid: it has a finite yield strength and behaves as Newtonian fluid beyond the yield strength. Although there are a lot of studies on the large scale complex craters by numerical simulations by using iSLAE, there is little studies to compare these simulations with laboratory experiments. Thus, the numerical results should be confirmed by the laboratory experiments to assure their numerical models. One of the most important points of the numerical model is rheological properties of the fluidized region and how it behaves during the crater formation process. Then, we try to study the crater formation process of fluidized material with various rheological properties such as yield strength and viscosity.
In this study, we used granular materials including various water contents in order to control the rheological properties of target. Glass beads with the size of 100 μm and quartz sand with the size of 100 μm were used for the target with the water contents from 0 to 24.5 wt.%, and we found that the pore space in the granular layer was completely filled with water at the content larger than 19.3 wt.%. The yield strength, Y, of the wet glass beads layer was measured by means of indentation tests and the obtained Y rapidly increased from 1kPa to 50kPa when the water content changed from 0 to 3wt.%, then it gradually increased from 50kPa to 100kPa until 17.5wt.%. Beyond the content of 17.5wt.%, the Y suddenly dropped below 5kPa until 19.5wt.%. Moreover, the relationship between the Y and the indentation speed for the wet glass beads layer with the content of 20wt.% was studied, and it was clarified that the Y of this saturated layer was proportional to the square root of indentation speed. We used this wet glass beads with various rheology for the high-velocity cratering experiments. The impact experiments were made by using a vertical type gas gun set at Kobe University, and the target box was set below a wind shield in a sample large chamber. The glass bead projectile with the size of 3mm was launched at the velocity of 170m/s, and the cratering process was observed by a high-speed digital video camera with the frame rate of $2x10^3$ FPS.
The crater shape was found to change with the water content: a bowl type for 0 to 3wt.%, a pit type with fractured rim for 3wt.% to 17.5wt.%, and a pit type with deformed rim for > 17.5wt.%. The high speed camera image was used to characterize the ejecta corresponding to the crater morphology. The bowl type crater was associated with a continuous ejecta curtain, and the pit type crater with a fractured rim was associated with many fragments composed of clumps. The pit type crater with a deformed rim formed small amount of ejecta and was associated with low velocity ejecta curtain undetached from the surface. The crater diameter was found to monotonically decrease with the water contents up to 18.3wt.% irrespective of the crater morphology, but the crater depth decreased until 15wt.% and then it rapidly increased from 15wt.% to 18.3wt.% corresponding to the pit type crater with a deformed rim. Thus, the depth to the diameter ratio could be classified into 3 region depending on the crater morphology: it simply increased from 0.1 to 0.5 for a bowl type, and it was a constant of 0.5 for a pit type with a fractured rim, and then it rapidly increased again for a pit type with a deformed rim. The crater depth could be controlled by the yield strength of the wet sand, but the crater diameter could not be controlled by the yield strength at the water content larger than 17.3wt.%. In this region, the wet sand showed non-newtonian behavior, thus this rheological property might cause the decrease of the crater diameter in

this region.

Keywords: Complex crater, Rheology, High-Velocity impact phenomena

The effect of sulfur on space weathering

*Hirokazu Tanaka[1], Sho Sasaki[1], Mizuki Okazaki[1], Takahiro Hiroi[2]

1. Department of Earth and Space Sciences, School of Science, Osaka University , 2. Department of Earth, Environmental and Planetary Sciences, Brown University

Space weathering alters surface optical properties on airless rocky bodies; the spectral darkening, reddening, and weakening of absorption bands are shown as for the optical changes. The cause of these changes is nanophase iron particles (np) generated by irradiation of solar wind or bombardment of micrometeorites. Although space weathering is also observed on the surface of Mercury, Messenger showed that there was a little iron, which was the main driver of space weathering, while there was more sulfur in weight abundance. Not only np but also sulfur or its compounds would contribute to space weathering. Okazaki et al. (2016) showed that addition iron sulfide to olivine samples had the effect of promoting space weathering. Moreover, SEM observation suggests that there is sulfur deposition on an olivine particle and which causes Mercury-like space weathering. In this study, we irradiated laser to the sample containing pure sulfur in order to simulate and examine the effect of sulfur on space weathering. First, we performed experiments of pulse laser irradiation to olivine and S mixture samples in a vacuum chamber. The samples were made with olivine and 10 weight % of S mixture (both particle size 45-75 m), and they were irradiated at 5 mJ. Moreover, we carried out additional thermal fatigue experiments to some of laser irradiated sample. After laser irradiation and/or thermal fatigue experiments, reflectance spectra (wavelength range 250-2500 nm) of these samples were measured by a spectrometer in order to examine alteration in optical properties.
The result of laser irradiation experiments showed that the spectra of samples including S reddened more than those without S. The result of thermal fatigue experiments showed that the spectra of samples including S changed complexly going with vaporization loss of S. It is confirmed that sulfur influence changes of optical properties in space weathering.

Performance report of solar wind ion irradiation equipment

*Yusuke Nakauchi[1], Toru Matsumoto[2], Masanao Abe[2,1], Akira Tsuchiyama[3], Aki Takigawa[3,5], Naoki Watanabe[4], Yuma Asada[3]

1. The Graduate University for Advanced Studies, 2. The Japan Aerospace Exploration Agency, 3. Kyoto University, 4. The Hakubi Center for Advanced Research, Kyoto University, 5. Hokkaido University

For understanding the evolution of the solar system, the material distribution in the early solar system is important. Meteorites provide large information on materials of the solar system, but they do not retain direct evidences for which parent body each meteorite came from.
The comparison between reflectance spectra of asteroids and meteorites suggest that the origins of almost all meteorites are asteroids. However, there are clear differences between reflectance spectra of asteroids and meteorites [references], which may be due to the space weathering on the surfaces of the asteroids. Recent studies proposed the importance of the influence of the solar wind implantation on the asteroidal surfaces in the near-Earth orbit [e.g. 1, 2]. Solar wind is composed of ~95% hydrogen, ~4% helium and other atoms [3]. However, space-weathering effects by low energy proton and helium ions consisting of the solar wind have not been understood well. In this study, we established ion beam irradiation equipment in ISAS/JAXA. This equipment is composed of an ion gun, main chamber (ion irradiation room), load lock chamber (sample preparation and FTIR measurement room), and FTIR. We can select ions with a specific mass and valence using the electric and magnetic fields. The maximum acceleration energy of ions is 5 keV. The reflection spectra of the irradiated samples can be measured without exposing the sample to the atmosphere. The optical path of FTIR can be purged with nitrogen. Therefore, the FTIR spectra of irradiated samples are obtained with minimized influences of adsorbed water and atmospheric fluctuations. In this presentation, we report the performance (e.g. beam current, beam shape) of ion beam irradiation equipment.

[1] C.M. Pieters et al., Science, 326(5952):568–572, 2009.
[2] T. Noguchi et al., MPS, 49(2):188–214, 2014.
[3] J.T. Gosling, Encyclopedia of the Solar System (Second Edition), pages 99 –116, 2007.

Keywords: solar wind, space weathering

Development of Exoplanet Observation System using ExoKyoto

Yosuke Yamashiki[1], Takao Doi[3], *Takanori Sasaki[2], Akihiro Yamanaka[5], Yuuki Saito[5], Shigeru Namiki[5], Keiya Murashima[5], Natsuki Hosono[1], Shota Notsu[2], Yuta Notsu[2], Kuroki Ryusuke[1], Hiroaki Sato[4], Fuuka Takagi[6]

1. Global Water Resources Assessment Laboratory - Yamashiki Laboratory Graduate School of Advanced Integrated Studies in Human Survivability Kyoto University, 2. Graduate School of Science, Kyoto University, 3. KYOTO UNIVERSITY UNIT OF SYNERGETIC STUDIES FOR SPACE, 4. Faculty of Engineering, Kyoto University, 5. Faculty of Science, Kyoto University, 6. Faculty of Agriculture, Kyoto University

An integrated database of confirmed exoplanets has been developed and launched as “ExoKyoto,” for the purpose of better comprehension of exoplanetary systems in different star systems. The HOSTSTAR module of the database includes not only host stars for confirmed exoplanets, but also over hundred thousands of stars existing in the star database listed in (HYG database). Each hoststar can be referred to in the catalogue with its habitable zone calculated, based on the observed/estimated star parameters. For outreach and observation support purpose, ExoKyoto possesses Stellar Windows, developed by the Xlib & Ggd module, and interfaces with GoogleSky for easy comprehension of those celestial bodies on a stellar map. Target stars can be identified and listed by using this database, based on the target magnitude, transit frequency, and photon decrease ratio by its transit. Using the developed exoplanet observation system on ExoKyoto, we performed some test observations at Kwasan Observatories, Kyoto University. We will show some preliminary results of the observations and introduce how to use the exoplanet observation system using ExoKyoto.

Extrasolar Planet’s Catalogue (ExoKyoto)
http://www.exoplanetkyoto.org

Keywords: Extrasolar Planets, Exoplanetkyoto, habitable zone

Atmospheric Dynamics on Non-Synchronized Tilted Exoplanets: Implications on Observed Thermal Light Curves

*Kazumasa Ohno[1], Xi Zhang[2]

1. Department of Earth and Planetary Science, Tokyo Institute of Technology, 2. Department of Earth and Planetary Science, University of California Santa Cruz

Various theoretical studies of atmospheric dynamics have investigated the dynamical structure on close-in synchronized exoplanets and succeeded to explain the phase curve observations. As the planets are farther away from their central stars, they are not likely to be tidally locked. Recent studies also begin to examine the atmospheric dynamics on non-synchronized exoplanets (e.g., Showman et al. 2015); however, they assume the planetary obliquity, the angle between orbital normal and planetary spin axis, is zero that is usually not true for non-synchronized planets.

In this study, we investigated the atmospheric dynamics on non-synchronized tilted exoplanets with a 2D general circulation model. We find that the temperature structure is considerably different from that on the synchronized exoplanets. Non-zero obliquities induce the temperature structure that is dominated by diurnal mean insolation if the radiative timescale is longer than rotation period but shorter than orbital period. The temperature is dominated by annual mean insolation if the radiative timescale is longer than both rotation and orbital periods. Seasonal variation as function of orbital phase is analyzed. We also predict the shape of observed thermal light curves for non-synchronized tilted exoplanets. Our prediction suggests that the amplitudes of light variation for high-obliquity exoplanets might be several times larger than that for the low-obliquity exoplanets but the differences depend on the parameters such as the radiative timescale and the line of sight from an observer. Furthermore, we find that the thermal light curves for tilted exoplanets might have a peak after the secondary eclipse if they are transiting, whereas for synchronized planets the phase curve peak always occurs before the secondary eclipse. Consequently, our results suggest that the planetary obliquity has the crucial impacts on the interpretations of observed phase curves for non-synchronized exoplanets.

Keywords: Exoplanets, Atmospheric Dynamics, Thermal Light Curve

Equilibrium chemical structure of extrasolar gas giant planets with various elemental abundance and temperature profiles

*Shota Notsu[1], Hideko Nomura[2], Catherine Walsh[3], Christian Eistrup[4]

1. Department of Astronomy, Graduate School of Science, Kyoto University, 2. Department of Earth and Planetary Science, Tokyo Institute of Technology, 3. School of Physics and Astronomy, University of Leeds, UK, 4. Leiden Observatory, Leiden University, The Netherlands

It is thought that difference in snowlines of oxygen- and carbon-bearing molecules, such as H_2O, CO, HCN, CO_2, will result in systematic variations in the C/O ratio both in the gas and ice. In addition, the C/O ratio of atomosphere of some exoplanets (e.g., Hot Jupiter) were measured by recent studies (e.g, Madhusudhan et al. 2011). Therefore, the planet forming regions could be confined through comparing the radial distributions of C/O ratio in disks and those of planetary atmospheres (e.g., Oberg et al. 2011, Eistrup et al. 2016).

In previous studies, We have calculated the chemical composition and the molecular line profiles in various protoplanetary disks, and have identified candidate molecular lines ranging from infrared to sub-millimeter wavelengths to locate the position of snowlines and C/O ratio distributions through future spectroscopic observations (e.g., Notsu et al. 2016, ApJ, 827, 113; 2017, ApJ, 836, 118).

In this study, first we calculated the physical structure of irradiated extrasolar gas giant planets using the analytic radiative equilibrium model in Guillot et al. (2010, A&A, 520, A27). Then, we calculated the chemical structure on equilibrium state of the gas giant planets. In these chemical calculations, we adopted various values of the distance from the central star, and elemental abundance (e.g., C, O, N), in order to investigate the relations between chemical structure of planetary atmospheres and their formation conditions in protoplanetary disks.

We found that as the values of temperatures in planetary atmosphere become smaller, the abundance of CH_4 become higher. In addition, as the values of C/O ratio become larger than the solar value, the abundance of CH_4 and HCN become higher in the lower atmospheres. In our talk, we will introduce the present calculational results, and will briefly comment the relations between the calculational results and recent observations.

Keywords: Extrasolar planet, Gas planetary atmosphere, Chemical equilibrium, C/O ratio, Snowline, Protoplanetary Disk

Simulation of the early Martian climate using a general circulation model, DRAMATIC MGCM: Impacts of thermal inertia

*Arihiro Kamada[1], Takeshi Kuroda[2], Yasumasa Kasaba[1], Naoki Terada[1]

1. Graduate School of Science, Tohoku University, 2. National Institute of Information and Communications Technology

There are many fluid traces on the Martian surface supposed to be made before ~3.8 billion years ago. If they were made by the liquid H_2O, the environment of the ancient Mars should be suitable for huge amount of liquid water, at least under higher temperature and larger atmospheric pressure than today. In order to reproduce such early Martian climate, several modeling studies have been performed so far. The solar insolation at that time is thought to be ~75% of today from a standard stellar evolution model. In this condition, a preceding study using the LMD Martian General Circulation Model (MGCM), with vertical 15 layers up to ~50 km altitude assuming the pure CO_2 atmosphere, showed that the surface temperature above 273 K could not be reproduced in the range of the surface pressure in 0.1 - 7 bars [Forget et al., 2013, hereafter F13], which is so-called the 'Early faint Sun paradox'.
In F13 the discussion of the effects of thermal inertia on the surface temperature was simplified, just describing the differences of results between the soil (surface albedo of ~0.22 in average and thermal inertia of 250 J $s^{-1/2}$ m^{-2} K^{-1}, hereafter the unit is omitted) and ice (surface albedo of 0.4 and thermal inertia of 1,000) surfaces. If ancient Martian surface was covered with wet and ice-free soil, the thermal inertia should become much larger than that of today, with the surface albedo of lower than 0.4 (the ground covered by ice). In this case, the results of surface temperature should be different from those which have been shown in F13.
From this point of view, we performed the simulations of the ancient Martian environment, especially focusing on the sensitivity of thermal inertia, using our improved MGCM, DRAMATIC (Dynamic, RAdiation, MAterial Transport and their mutual InteraCtions) [e.g., Kuroda et al., 2005]. We assumed the pure CO_2 atmosphere as F13. We have implemented the radiative effects of CO_2 gas assuming the sub-Lorentzian profile [Fukabori et al., 1986] and considering also the collision induced absorptions [Gruszka and Borysow, 1997]. For the comparison with F13’ s results, the obliquity, eccentricity, surface albedo and thermal inertia are set to be the same as their standard simulation. Also the vertical coordinate of the model is set to 15 layers to ~50 km altitude, as well as F13, and horizontal resolution is set to 64x32 (5.625deg latitude by 5.625deg longitude). The radiative effects of CO_2 ice clouds are also considered in solar and infrared wavelengths as well as F13, although the radiative effects of dust are not considered.
At first, in order to check the validity of our model, we simulated with globally constant thermal inertia of 250 (soil) for the globally averaged surface pressure of 0.1 –3 bars (realistic pressure range of early Mars). The results showed that annual mean surface temperature in the equilibrium state increased with surface pressure, but the annual mean temperature was ~225 K for 2 bars and ~237 K for 3 bars, far below the H_2O melting point. The infrared optical depth of CO_2 ice clouds reached the highest value of τ ~1.4 for the surface pressure of 1.5 bars, probably because of the profiles of CO_2 condensation temperature and simulated annual-mean temperature against surface pressure which indicated the most favorable production of CO_2 ice clouds at ~1.5 bars. The radiative effects of CO_2 ice clouds affect to increase the global mean temperature for several Kelvins in maximum, while ~10 K in F13.
Next, we simulated with globally constant thermal inertia of between 1,000 (ice) and 5,000 (wet soil assumption) for the surface pressure of 2 and 3 bars. The results showed that annual mean surface temperature in the equilibrium state greatly increased with increased thermal inertia. Daily mean surface temperatures in northern low- and mid-latitudes and Hellas basin, where are in low altitude and

considered to be the places of ancient ocean/lake, are above 273 K almost throughout the Martian year for 3 bars and thermal inertia of 5,000.
Our results suggest that the surface conditions could be the key of the existence of liquid water in early Mars. The surface with high thermal inertia may be able to produce the surface temperature higher enough to keep liquid water even with the pure CO_2 atmosphere under the solar insolation which was ~75% of today.

Keywords: Mars, paleoclimate, thermal inertia, GCM, sub-Lorentzian, collision induced absorption

Stratified hybrid-type proto-atmosphere on accreting Mars

*Hiroaki Saito[1], Kiyoshi Kuramoto[1]

1. Department of Cosmosciences, Graduate School of Sciences, Hokkaido University

The precise Hf-W chronology suggests that Mars reached about half of its present mass within the 1.8 ± 1.0 Myr or less after the formation of CAI with core-mantle differentiation (Dauphas and Pourmand, 2011). Since this timescale is much shorter than the estimated lifetime of the solar nebula, the accretion of Mars mostly proceeded within the solar nebula. On the other hand, the energy released by planetesimals collisions becomes large enough to induce degassing of the volatile compounds such as H_2O when the proto-Mars gets bigger than the lunar size (0.1 M_M). Therefore, growing Mars may have a proto-atmosphere that consists of nebula gas and degassed gas.

We analyze the thermal structure of stratified hybrid-type proto-atmosphere where the solar nebula component dominates the upper layer, and the degassed component dominates the lower layer, by developing a 1D radiative-equilibrium model. Provided that the building blocks of Mars are described by the two-component model, which contains 4 wt% of volatiles, a hot proto-atmosphere is formed with the surface temperature exceeding the melting point of rocks (1500K) when accretion time is within 4 Myr. This suggests that the core-mantle differentiation efficiently proceeds due to the formation of a magma ocean produced by the atmospheric blanketing effect.

However, there is a possibility that the proto-atmosphere may be mixed due to convection or molecular diffusion. The mixing of the proto-atmosphere possibly changes the thermal structure of the proto-atmosphere. There is also uncertainty for the volatile concentration in the building blocks.

In this study, we investigate condition for keeping atmospheric stratification by comparing the level of the compositional boundary (CB) and the tropopause, and the accretion time and mass exchange time scale controlled by molecular diffusion. The accretion times is taken from 1 –6 Myr as the chronology suggests. In the case of the volatile concentration is 4 wt%, we found that the level of the CB is always above the tropopause for any accretion times and proto-Mars mass, which means convective mixing between the solar nebula layer and degassed component layer does not occur. Moreover, the mass exchange time scale is about 10^2 times longer than the accretion time. Thus the mixing by molecular diffusion is unlikely to occur. On the other hand, when the volatile concentration is less than 2 wt%, the level of the tropopause is located above the level of the CB, and therefore the convective mixing occurs across the solar nebula layer and the degassed component layer. The resultant changes in the thermal structure of the proto-atmosphere are now under study.

Keywords: Proto Mars, Proto-Atmpsphere

Increase in ferrous ion by soaking basalt in acid water solution and UV rays

*Nobuo Komori[1]

1. Ota Ward Kamata Junior High School

Recent proven by the Mars explorer, it was shown that there was an ocean on Mars 43 billion years ago. That ocean might have been made of acid. Having this ocean as a precondition I did two following experiments to test this theory about mars.
In the first experiment, I measured density of ferrous ion which went into two kinds of solution ;solution neutralizing sulfuric and basalt: hydrochloric acid and basalt.
My result was that about 5 times more ferrous ion dissolved in pH1 hydrochloric acid than in pH2. In the second experiment I measured the density of ferrous ion in the case of going into solution when fayalite and basalt were soaked in purified water, hydrochloric acid, and sulfuric. And the other case was in the same condition with UV irradiated. Results show the denstiy of ferrous ion in the case of UV irradiation was 1.5 times higher than non UV irradiation.
As a result of these experimental results, a large quantity of ferrous ion might have been dissolved in Mar’ s ocean because of the neutralization of the acid by rocks such as basalt. Furthermore, dissolved ferrous ion might have been increased by solar ultraviolet rays C.

Keywords: ultraviolet rays, ferrous ion, fayalite, basalt, acid aqueous solution

Origin of Solar system is explored by the question "Why?". Operation of Planet was elucidated by Newton's law. “Multi-impact hypothesis” that unifiedly explains Origins of Asteroid belt, Moon, Jupiter's red spot, using Abduction.

*Akira Taneko[1]

1. SEED SCIENCE Lab.

Proof by abduction (a means of exploring the origin to the past where neither the earth nor human beings are formed), if it can explain the current multiple mystery in a unified manner with a hypothesis having a physical meaning, the evolution and history of Yuichi's solar system I understand that the validity of the hypothesis was supported as the truth verified by.The hypothesis which can show the basis of the origin is groundbreaking as an effective means of the origin problem of geophysics which can neither experiment nor theoretically calculate.

In Multi-Impact Hypothesis, *CERRA is formed at Cerres position in Bode's rule, the eccentricity increases by Jupiter perturbation.* **Sera split about 4 billion years ago by Jupiter's tidal power and became Origin of Aasteroid belt.**
Furthermore, Mantle fragments crashed into Earth (12.4 km / s, 36.5 degrees: value derived from Hypothesis) and Moon was formed at Current distance (60RE). Collision position was Pacific Ocean and Crust peeling trace was Isostasy and became Darwin uplift. Multi-Impact of Multiple iProof by abduction (a means of exploring the origin to the past where neither the earth nor human beings are formed), if it can explain the current multiple mystery in a unified manner with a hypothesis having a physical meaning, the evolution and history of Yuichi's solar system I understand that the validity of the hypothesis was supported as the truth verified by.mpact is Origin of extinction of species, cause Mantle cracks and Formation of plate boundary, It is also Origin of deep ocean floor and Earth twin frequency formation. Earth rotation and Earth core eccentricity and effect of inertial efficiency unbalance compensation were shown as driving force of plate tectonics, Wegener's continental drift theory and ocean floor update theory etc.
Furthermore, Origins of Pacific arcuate archipelago and back arc basin, Mantle exfoliation and Isostasy due to collision, Pressing of Concave plate basin and Convex plate are Origins of mutual slip between Origins of Average depth of 5 km.
Driving force of plate tectonics is due to Inertial efficiency of Earth due to imbalance due to Mantle collision peeling and equalization due to Direction of rotation of Earth. Plate boundary is Mantle crack at Time of collision, Melting point drops due to Pressure decrease and Mantle melts.

Keywords: Elucidation of origin by abduction, actial proof by one-time evolution, Proof of Titius Bode's Law, Mechanism of Accumulation, Origin of the moon, Origin of asteroid belt and meteorite, Origin of Jupiter Large Red Spot, Origins of deep ocean floor

The Origin of The Moon and The deep sea floor bottom and Plate-Tectonics elucidated with Multi-Impact Hypothesis.

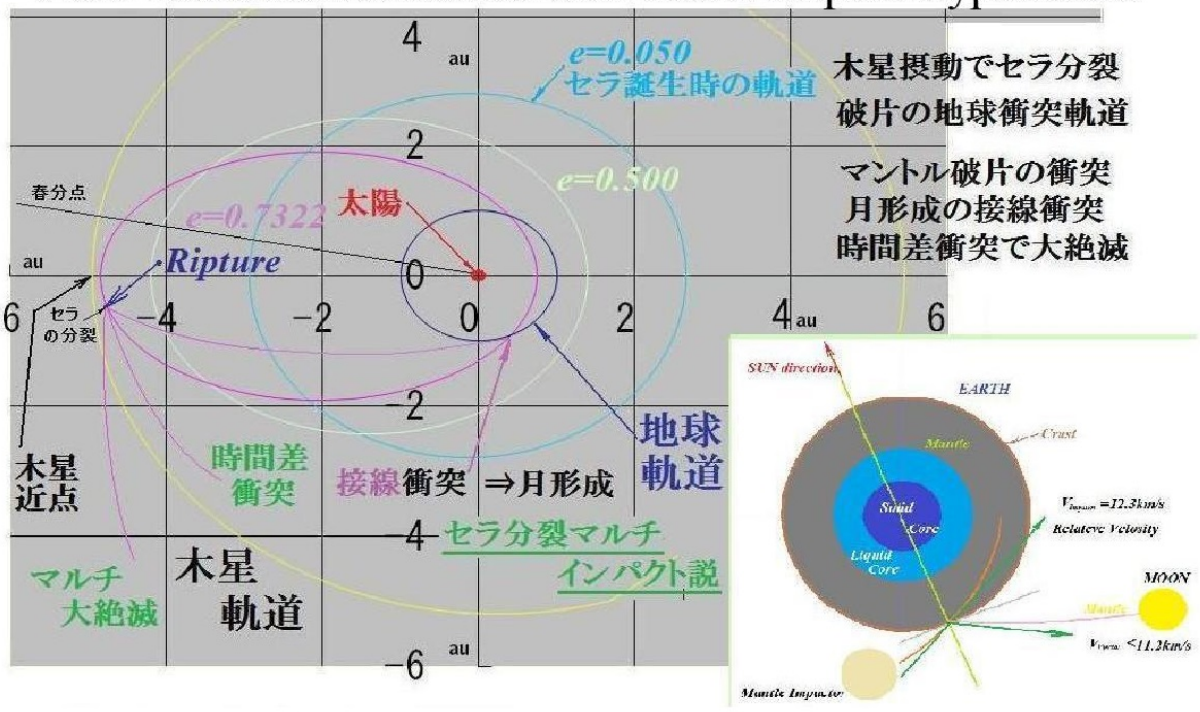

O8-08 The Origin of the Deep Ocean Floor and the Plate-Tectonics, Elucidation of the Driving Force, The Origin of the Moon and the Earth Deep Ocean Floor with Multi-Impact Hypothesis *2016 9-14*

8. プレートの駆動力,同じ密度のプレートが上下に重なる理由

8.1. プレートの駆動力は謎であった. ①.マントル対流仮説(.ホームズ)
②.前引き,後押し仮説 ③.リソスフェア厚さ傾斜仮説 ④.プリューム仮説
⑤. 慣性モーメントアンバランス解消偶力説 (本仮説) 偏芯の解消偶力.
マルチインパクト仮説で地殻プレートが図Aの状態⇒図Bの均質安定状態.

8.2. 同じ密度のプレートが他方の下に潜り込んで,海溝と和達・ベニオフ帯を形成するメカニズムの謎も有った. 衝突剥離時のアイソスタシーで凹海盆 α.

が形成された.
凸プレートと,凹プレートが押し合うと,凸プレートが折れ曲がって,凹プレートの下に潜り込む. β.
更に深く和達・ベニオフ帯を形成して,地震発生面に成る.